Magnetic and Non Magnetic Copper Sulfide Nanoparticles: Synthesis, Characterization and Environmental Application

A dissertation submitted to the Department of Chemistry, Quaid-i-Azam University, Islamabad, in partial fulfillment of the requirements for the degree of

Master of Philosophy

In

Inorganic/Analytical Chemistry

By

Noor ul Ain

Department of Chemistry
Quaid-i-Azam University
Islamabad
2015

DECLARATION

It is certified that all the experimental work was performed in Inorganic Chemistry Laboratory, Department of Chemistry, Quaid-i-Azam University, Islamabad, Pakistan.

To the best of my knowledge, the work is original and has never been presented by any other person at any platform or for the evaluation of M.Phil. Thesis.

Noor-ul-Ain

Noor ul Ain
Quaid-i-Azam University,
Islamabad,   Pakistan.
2015

This is to certify that this dissertation entitled *"Magnetic and non-magnetic copper sulfide nanoparticles: synthesis, characterization and environmental application"* submitted by *Ms. Noor ul Ain,* is accepted in its present form by the Department of Chemistry, Quaid-i-Azam University, Islamabad, as satisfying the dissertation requirements for the degree of *Master of Philosophy in Analytical/Inorganic Chemistry*

External Examiner:

Prof. Dr. Mrs. Uzaira Rafique
Dean Faculty of Science & Technology
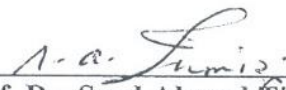Fatima Jinnah Women University
Rawalpindi

Supervisor:

Dr. Zia ur Rahman
Department of Chemistry
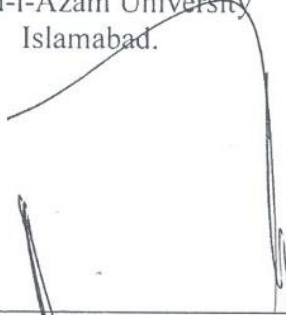Quaid-i-Azam University
Islamabad.

Head of Section:

Prof. Dr. Syed Ahmed Tirmizi
Department of Chemistry
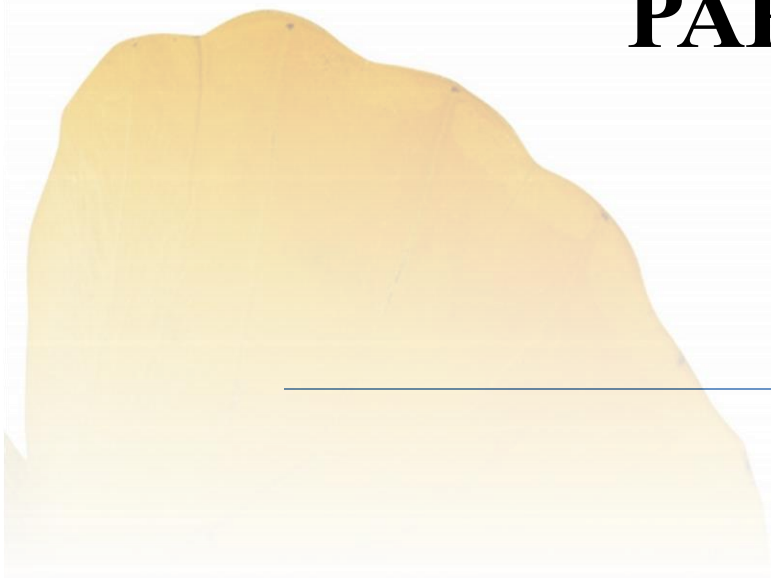Quaid-i-Azam University
Islamabad.

Chairman:

Prof. Dr. Amin Badshah (*TI*)
Department of Chemistry
Quaid-i-Azam University
Islamabad

DEDICATED TO MY PARENTS

ACKNOWLEDGEMENTS

Table of Contents

Abstract

A series of crystalline brown colored copper complexes $C_{36}H_{38}N_4S_4Cu$ (1), $C_{26}H_{32}N_2S_4Cu$ (2) and $C_{14}H_{26}N_4O_2S_4Cu$ (3) were prepared by simple chemical reactions. These complexes were characterized by melting points and IR (Infra-Red Spectroscopy). Solvothermal method was used for the formation of nanoparticles. These copper complexes were used as single source precursors. Ethylenediamine and octylamine were used as solvents. All synthesized copper sulfide nanoparticles were hexagonal in shape. Copper sulfide nanoparticles synthesized using octylamine as solvent were small and more crystalline as compared to those prepared by ethylenediamine. The size, shape, phase purity, crystallinity and elemental composition was determined by UV, XRD (X-Ray Diffraction), EDS (Energy Dispersive X-Ray) and TEM (Transmission Electron Microscopy). The crystallinity of the sample was determined by SAED (Selected Area Electron Diffraction). Photocatalytic activity of CuS was studied by degrading an environmental pollutant Congo red in dark, UV and sunlight. Synthesized copper sulfide nanoparticles have shown excellent photocatalytic activity better activity than previously reported in literature.

CHAPTER 1

INTRODUCTION

1.1. Applications of nanotechnology

Nanotechnology was emerged in 1980s. It was emerged after the invention of scanning electron microscope in 1981 and fullerence in 1985. The commercial applications of nanotechnology began in early 2000. Although nanotechnology is a recent development but it took very long time to develop its central concepts.

Nanoscience is the study of those materials whose size range between 1-100 nm. In nanotechnology matter is studied at atomic and molecular level. Nanotechnology is currently gaining attention of people because of its high impact on our lives as well as on our economy [1]. Nanoparticles have very fascinating and interesting properties which are not found in the bulk materials. Nanoparticles have surface effects and quantum mechanical effects due to which they are used to produce medical, optical and electronic devices [2]. Nanotechnology includes every science that operates at nanoscale. Royal society has defined nanotechnology as "Nanotechnology is the design, characterization, production and application of structures, devices and systems by controlling shape and size at nanometer scale" [3]. It is considered that nanotechnology brought an industrial revolution and have a great impact on our lives and economy [4]. There are many fields in which nanotechnology is excelling day by day. These fields include medicine, information technologies, biotechnologies, energy production and storage, material technologies, manufacturing, instrumentation, environmental applications and security [5]. These unique properties of nanoparticles are due to the reason that they have high surface to volume ratio [6]. This increased surface to volume ratio results in the increased interaction with the surface and hence can be used as catalysts.

Nanotechnology was firstly used in stained glass windows which were used in churches in medieval Europe. Nanoparticles have improved magnetic, conducting and

reflecting properties. Some of the applications of these materials are highlighted in Fig 1.1.

Fig. 1.1: Innovative Applications of Nanotechnology

Sun is an appealing energy source but conversion of solar energy into electricity is very expensive. Nanotechnology has provided efficient and low cost method for converting solar energy into electricity. Researchers are now working hard to produce low cost solar cells by nanotechnologies that are not only transparent but also flexible. These solar cells are able to collect the solar energy from entire building rather than just roof.

Nanoparticles are used as biological labels. Nanoparticles have the same size as of a protein that's why they are considered suitable for bio tagging or bio labeling [7]. We have to do biological or molecular coating or to attach a bioinorganic interface with nanoparticles. After doing this nanoparticle will interact with biological target. Biological coatings include antibodies or biopolymers like collagen [8].

Nanoparticles can be used in cancer therapy. Photodynamic cancer therapy is used for the destruction of cancer cells but it is cytotoxic. A special dye is used in this method to destroy cancer cells but the demerit of this method is that the dye which is left after being absorbed by the cancer cells migrate to the skin and eyes and make them sensitive towards sunlight. In cancer therapy porous nanoparticle is used. This dye only remains inside the nanoparticles and do not migrate to other body parts [9].

Nanomaterials are classified into three types on the basis of dimensions. These types are surface films (one dimensional nanoparticles), strands or fibres (two dimensional nanoparticles) and particles (three dimensional). They can exist in single, fused, aggregated or agglomerated forms with spherical, tubular, and irregular shapes (Fig. 1.2).
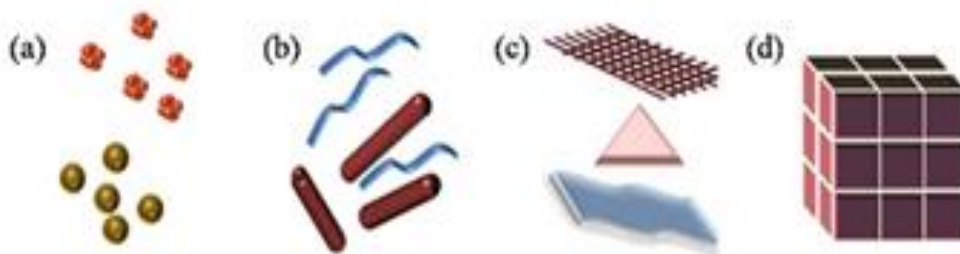
Fig.1.2: Classification of nanomaterials (a) 0D clusters and spheres (b) 1D nanofibers, rods and wires (c) 2D films, plates and networks (d)3D nanomaterials

1.2. Copper sulfide nanoparticles

Copper sulfides are the chemical compounds having general formula Cu_xS_y. Copper sulfide nanoparticles are now a days gaining a lot of interest in Nano science due to its fascinating physico-chemical properties. By varying the stoichiometries of copper to sulfur in CuS, the band gap and the electronic and crystal structures can be varied. Copper sulfide nanoparticles in various stoichiometries have been produced, like Cu_2S (chalcocite), CuS (Covelite), $Cu_{1.97}S$ (djurleite), $Cu_{1.8}S$ (digenite) and $Cu_{1.4}S$ (anilite) [10].

In copper sulfide nanoparticles monovalent state is more preferred over divalent state because of its extensive favorable properties. Monovalent copper sulfide nanoparticles can be used as semiconductors. CuS and CuS_2 are the most common forms. CuS mono sulfide is metallic, diamagnetic conductor and it also becomes superconductive below 1.62K. On the other hand copper disulfide CuS_2 is a *p*-type metallic conductor. Copper disulfide has temperature independent paramagnetic property and it becomes superconductive below 1.5 K.

1.3. Previous known methods for preparation of copper sulfide nanoparticles and their limitations

Copper sulfide nanoparticles are prepared by many methods like hydrothermal methods, micro emulsion methods, ultrasonic method and solvothermal methods etc.

In ultrasonic method copper precursor is first dissolved in propylene glycol then Na_2SO_3 and HCl are added to the precursor solution. Thiosemicarbazide (TSC) is then added to the above solution and stirred for some time and then the mixture is irradiated with ultrasound at 100°C. The power and time are varied. Copper sulfide nanoparticles in the form of precipitate are obtained which is separated by centrifugation [11]. This method requires ultrasonic ray's source.

In hydrothermal method metal salt like $CuSO_4.5H_2O$ is dissolved in distilled water along with $Na_2S_2O_3.5H_2O$ and $(H_3NO)_2. H_2SO_4$. It is then put in stainless steel autoclave under stirring at 200 $^{\circ}$C for 90 min. The precipitates of copper sulfide are obtained which are then washed and dried [12]. There are many disadvantages of hydrothermal process. The instrument used is expensive, the reaction is carried out in autoclave that's why it is difficult to monitor reaction, prior knowledge on solubility of starting material is required, hydrothermal slurries are potentially corrosive and accidental explosion of high pressure vessel cannot be ruled out.

In micro emulsion method stock solution is prepared by dissolving the copper salt in water. Surfactant, *n*-hexanol, cyclohexane and stock solution are mixed in a definite ratio to prepare micro emulsion. The value of *w* (aspect ratio i-e water to surfactant molar ratio) is fixed at 9. The solution is stirred at room temperature until the solution became transparent. The micro emulsion is then bubbled with N_2 under an aerobic environment. The micro emulsion is then irradiated in a field of ^{60}Co γ source for 16 h and 40 min with absorbed dosage of 40 kGy [13]. The drawbacks associated with nanoparticles obtained via micro emulsion methods are lesser quality nanoparticles, wider size distribution, particles exhibit long wavelength, broad spectrum, have defects and are not tunable.

In polyol method an appropriate amount of metal salt and thiourea are taken in a round bottom flask. Glycol solution is then added into it and stirred for some time. This solution is then refluxed along with heating for about 0.5-2 hours. Solution is then

cooled, filtered and washed. At last it is vacuum dried at 601°C for about 3 hours [14]. There are many disadvantages associated with this method. Large amount of polyhydroxy alcohol is required, choosing of the suitable polyhydroxy alcohol for individual processes, collecting and purifying of the intermediate particles are complicated.

In wet chemical method of copper sulfide synthesis CuCl is stirred in Milli-Q (Millipore Corporation) ultra-pure water for some time. TG (Thioglycerol) is added as a capping agent. This suspension is stirred for about 2 hours at room temperature. As a result of this complex chemical networks are formed between copper and TG. After 2 hours of time duration Na_2S in Milli-Q water is added drop wise into above suspension with continuous stirring at room temperature. The precipitates are allowed to settle in fume hood. The supernatant liquid is decanted and particles are again dispersed in Milli-Q water and put on stirring for 2 hours [15].

In sol gel method several transition metal halides are made to react with organic sulfur sources in CH_2Cl_2. The reactions are done at room temperature under reflux. The product obtained was amorphous and can be made crystalline by heating [16]. The disadvantages associated with sol gel method are raw materials for this process are expensive as compared to mineral based metal ion sources, products would contain high carbon content when organic reagents are used in preparative steps and this would inhibit densification during sintering. Since several steps are involved, close monitoring of the process is needed.

1.3.1 Solvothermal process

Solvothermal reaction is a reaction that involves the solvent either in subcritical or supercritical conditions [17]. Solvothermal is a general term which is used collectively for all types of solvents. In Solvothermal reactions solvent acts as chemical component and it helps to enhance the reaction due to its physico-chemical properties. When water is used as a solvent then the process is termed as hydrothermal method whereas in case of Solvothermal reactions solvents like hydrogen sulfide, benzene and ammonia etc. are used. Solvothermal reactions can produce sulfides, nitrides and carbides etc. Solvents provide milder and friendlier conditions for the reaction. This method is used for the preparation of nanoparticles, polymers, ceramics and semiconductors. The solvothermal process needs pressure between 1 atm and 10,000

atm and the temperature range is between 100ºC and 1000ºC. These conditions results in the good interaction of the precursors with solvent. These processes can produce many geometries like thin films, bulk powder, single crystal and nanoparticles. Quantum dots can be produced by Solvothermal route by controlling concentration, reaction time and temperature. Many factors both chemical and thermodynamic affect the Solvothermal reactions. Chemical factors include the chemical nature of the solvent, the physico-chemical properties of the solvent, the nature of the precursors and the experimental conditions. Thermodynamic factors include temperature and pressure.

1.3.1.1 Effect of solvent on solvothermal process

Many solvents are used in Solvothermal process. Solvent is in liquid phase and it effects the reaction due to its physiochemical properties. Solvent effect the speed of the reaction and thus controls the concentration of the product. It also helps to enhance the coordination of solvated species and induce specific structures. Those solvents which favors the formation of intermediates will slow down the kinetics of the reaction and will result in thermodynamically stable product. Solvents like ethylenediamine and water slow down the kinetics and forms thermodynamically stable product. Contrary to it solvents like tetrahydrofuran and benzene do not favors the formation of intermediates. They fasten the kinetics of reaction and as a result do not form thermodynamically stable product.

i. Effect of ethylenediamine on copper sulfide nanoparticles

In case of ethylenediamine Cu_2S is formed. This is due to the reason that ethylenediamine results in the reduction of Cu(II) to Cu(I). This reducing property of the amine solvent usually increases with the increase in temperature and pressure. Ethylenediamine also has strong polarity and strong chelating ability. Alkyl amine also has a role in lowering the temperature of alkyldithiocarbamates from 170ºC to 125ºC. The boiling points of the solvents should be greater than 100 ºC. If the temperature of the reaction is below the decomposition temperature of precursor then aggregated product will be formed. The metal complex usually becomes unstable in the presence of chelating ligand. This strong chelating solvent (ethylenediamine) will replace the primary ligand and will form stable intermediate chelate complex. This intermediate ligand complex will act as a reaction template and will produce mono dispersed copper sulfide nanoparticles [18].

ii.   Effect of octylamine on copper sulfide nanoparticles

The ligands play a very important role in controlling the stability and sulfuration speed of copper sulfide nanoparticles. Alkylamines speed up a reaction and without them the sulfuration reaction would become very slow and irregular shaped nanoparticles are obtained. Octylamine binds with the copper dithiocarbamates to form five or six coordinated complex. With the increase in the temperature coordinated octylamine will go to the electron deficient thiocarbonyl carbon of the dithiocarbamate ligand and form a symmetric intermediate. Proton migration takes place and upon condensation hydrogen sulfide gas is released. Alkyl substituted thiourea is formed along with copper sulfide nanoparticles [19].

1.3.1.2 Effect of physicochemical properties of the solvent

The physico chemical properties of the solvent can be enhanced by using mixture of solvents. Due to this, product with enhanced electrical conductivity and transparency are formed [20].

1.3.1.3 Effect of nature of precursors

Precursors play a very important role in controlling the morphology of the particles. Different types of precursors are used in the history and their effect on morphology of particles was studied. By changing the concentration of the precursors the size of the nanocrystals increases. Dithiocarbamate precursors are also involved in the reduction of copper from +2 to +1 oxidation state. The reduction is also confirmed by the fact that $Cu_{2-x}S$ NCs without dithiocarbamates have more oxidized S content. If dithiocarbamates are used in excess then they will form (–Cu–DT–) n complexes, which compete with sulfuration reaction.

1.3.1.4 Effect of temperature

By controlling the temperature various factors can be controlled. By varying the temperature we can control the solubility of the precursor, kinetics of the reaction, stability of the reactants, composition of the solvent and formal oxidation state of the transition metal. Moreover, by increasing temperature decomposition of the solvent can be enhanced as a result better crystalline particles are obtained.

1.3.1.5 Effect of pressure

In solvothermal processes pressure also plays its role. Pressure can stabilize the more densely packed structures. If the range of pressure is high then the thermal stability domain of the reactant will also increase. By varying the pressure the kinetics and thermal stability of the reaction can be enhanced. This was due to the success of solvothermal process that many scientists have made use of this method to produce nanoparticles. Suja, Geetha and Ramesh have prepared copper sulfide (CuS) nanoparticles by using copper nitrate trihydrate, thiourea, ethanol and ethylene glycol (solvent). Size controlled and stabilized product was formed by using this method [21]. Liu, Liang, Qian, et al prepared copper sulfide nanoparticles by using copper thiolate and thioacetamide. The dodecanethiol as a solvent and then particles were precipitated by using ethanol [22]. Gorai, Ganguli, and Chaudhuri prepared copper sulfide nanoparticles by using copper nitrate and thiourea. They used ethylenediamine and ethylene glycol as solvents. The reaction was done in autoclave at 130ºC for about 12 hours [23].Another research group have synthesized copper sulfide nanoparticles by decomposing copper(II) diethyldithiocarbamates using trioctylphosphine as a solvent. The reaction was done under inert conditions and the temperature was maintained at 240 ºC – 250 ºC [24]. The complex, $[Cu(SMDTC)Cl_2]$, (where SMDTC is S-methyldithiocarbazate) was decomposed using many solvents like ethylene glycol, ethylenediamine, HMDA (Hexamethylenediamine) and HA (hyaluronic acid). The temperature was varied from solvent to solvent [25].

The types of solvent we choose closely depend on the chemical composition of the resulting desired material and the physiochemical process modifies the chemical reaction. There are three goals of solvothermal crystal growth. These goals are obtaining product at low temperature [26], preparing product with less defects [27-28] and developing new crystal-growth processes of non-oxides (nitrides, sulfides…)

Alkylamines were used as solvent to obtained crystalline, defect free, well defined, easily tunable and narrow size particles [29]. Alkylamines strongly affect the size of the nanoparticles; amines with bulky hydrophobic groups are weak ligands towards copper and sulphur species. By increasing number of alkyl chains increase sulfuration, and as a consequence particle size decreases [30].

1.4. Single source precursors

Single source precursor involves those compounds that contain all the essential elements that are required for the synthesis of nanoparticles [31]. Single source precursor are generally volatile, stable under moisture [32], contains preformed bonds that results in material with less defects and good stoichiometry [33] and thermal decomposition yield handsome amount of particles [34]. Moreover, the purification of product is easy because only precursor is involved in the reaction. Single source precursors are very efficient and inexpensive means of producing semiconductor nanoparticles. The use of single source precursors in the formation of nanowires has also solved the reactivity based problems. By controlling the concentration of single source precursors we can control the morphology of nanoparticles. Many copper dithiocarbamates complexes have been synthesized and are used as single source precursors. One of the examples of copper dithiocarbamates complex is as following (Fig. 1.3).
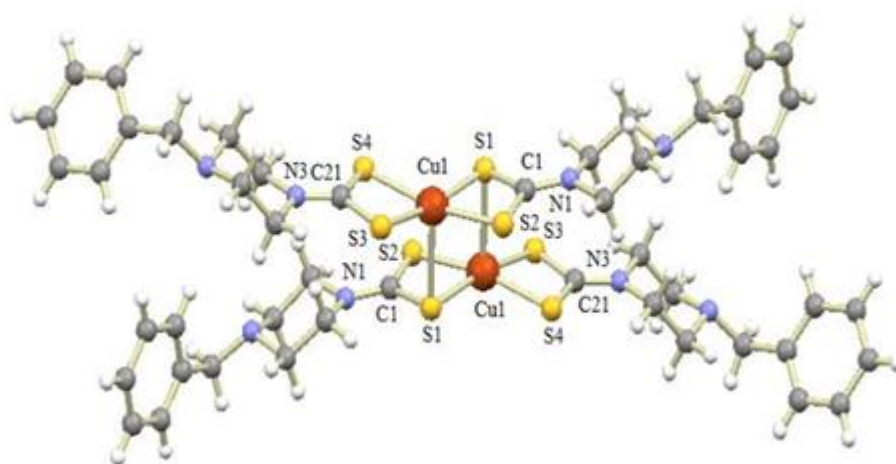
Fig. 1.3: Di-µ-this-tetrakis (4-benzylpiperazine-1-carbodithioato) dicopper (II)

If we increase the concentration then the size of nanocrystals not only becomes larger but also the level of branching increases in the crystal [35].

High purity copper sulfide nanoparticles are formed by the use of dithiocarbamates. Asymmetrical dithiocarbamates are more efficient in preparing nanoparticles than symmetrical dithiocarbamates. This is because they are sufficiently more volatile. The use of dithiocarbamates as single source precursors depend both on

the nature of the alkyl group as well as dithiocarbamates groups [36] .One more reason behind the use of dithiocarbamates as single source precursors is that they are moisture and air insensitive, less toxic and are easy to synthesize and handle. Temperature also has a great influence on the nanoparticles. We can use high temperature to produce defect free nanoparticles in case of single source precursors (dithiocarbamates) [37].

If the heating of solution is done at high temperature then nanocrystals with less defects are obtained. Better crystallinity is obtained in this case. This has photovoltaic applications, this is because the carriers which are produced by absorption of light have longer free carrier lifetime. Due to less combination of free carriers at defects more current is produced. Single source precursors are less noxious than other precursors. All these advantages of single source precursors make them suitable for nanoparticles formation. Many scientists have made use of single source precursors to produce copper sulfide nanoparticles. Ngo et al. had made use of Cu(II) dialkyldithiocarbamates as single source precursor to form copper sulfide nanoparticles. The copper sulfide nanoparticles formed by this had superconducting nature. [38] Another group had used substituted dithiocarbamates [Cu(py)$_2$(dedtc)$_2$] as a single source to produce copper sulfide nanoparticles [39].

Ilan Jen-La Plante, Tahani W. Zeid, Peidong Yang and Taleb Mokari had made use copper(II) diethyldithiocarbamates, Cu(II)[S$_2$CNC$_4$H$_{10}$]$_2$, to prepare copper sulfide nanoparticles using trioctylphosphine as a solvent. The reaction conditions were inert with temperature from 240-250°C. The concentration of single source precursors used determines the composition of copper sulfide nanoparticles [40]. A.K. Sharma had made use of dihexyldithiocarbamates and dioctyldithiocarbamtes as single source precursors to synthesize cuprous sulfide nanoparticles [41]. Nomura et al prepared Cu$_2$S from decomposition of copper dialkyldithiocarbamates, Cu(S$_2$CNR$_2$)$_2$, here R = ethyl, butyl and octyl etc, at 320°C [42]. So we can say that this is due to the advantages of copper dithiocarbamates that they are used as source to produce nanoparticles.

1.5. Applications of Cu$_x$S$_y$ nanoparticles according to band gap

Copper sulfide is a *p*-type semiconductor with a direct band gap of 1.2 to 2 ev. In a study it was found that copper sulfide nanowires who are having the size of 2.5 and 1.7 nm have very great aspect ratio (water to surfactant molar ratio). The band energies

are expected in the range of 3.47 to 3.69 eV. There is a great quantum effect in this range and these nanoparticles can be used in photovoltaic applications [43].

Those copper sulfide nanoparticles that have the band gap of about 2.2 eV found its application in photocatalytic mineralization of a number of dyes. These dyes are malachite green, methyl red, methyl orange and eosin [44].

The copper sulfide nanoparticles which have the band gap from 1.8 to 2eV found its applications in electro conductivity. They are highly transparent and electro conductive that's why they are used as highly conductive top electrodes. Copper sulfide (Cu_2S) films are deposited on the surface of the polyester film to form an electro conductive surface [45]. The layered structure of copper sulfide consist of copper atoms sandwiched between hexagonally packed sulfur atoms. Due to this crystallographic feature, they allow for the intercalation and reaction of alkali metal ions in between S-Cu-S layers. This makes copper sulfide nanoparticles a very good promising material for lithium ion battery [46].

In medical field the role of copper sulfide nanoparticles is to introduce new and novel technologies. DNA sequence is essential in many fields like analysis of genes, tests for disease diagnosis, drug screening and many more. Chemiluminescence detection based on nanomaterials is now days used for determining DNA hybridization. Classical methods are different from the new methods in that they involve the luminescence of the enzymes attached to the probe DNA upon hybridization to the target DNA [47]. As compared to these classical methods, the new methods involve the luminescence of the semiconductor nanoparticles attached to DNA. This new technique is better than previous classical ones because of two reasons: Poor stability of enzymes and low detection sensitivity. The instability of Ag^+ and Au^{3+} in aqueous solutions remains a disadvantage. $Cu^{2+,}$ on the other hand, is highly soluble in water and much less expensive for DNA sequence detection.

Copper sulfide nanoparticles are also used as bio labels. For producing glucose sensors glassy carbon electrodes were used. These electrodes were coated with multi-walled carbon nanotubes (MWNTs) and modified with single crystalline copper (I) sulfide (Cu_2S) nanocrystals. These copper (I) sulfide nanocrystals which were used for modifications have different morphologies. These sensors were more sensitive to H_2O_2 as compared to conventional GOX-based sensors. The H_2O_2 was produced during

glucose oxidation by GOX (Glucose oxidase). The detection limit of these new sensors was 50 nM whereas the detection limit of conventional GOX-based sensors was 10 μM. [48].

Copper sulfide nanoparticles also have its applications (Fig. 1.4) in photovoltaic cells. When these nanoparticles were inserted into photovoltaic cells the efficiency of cells increased by 1.6%. This technique has opened a new path for low cost power conversion in near future [49]. The band gap between 3.47 eV to 3.69 eV is well suited for use in photovoltaic cells. This is because this band gap show stronger quantum size effect and have high potential for use as photovoltaic cells [50].
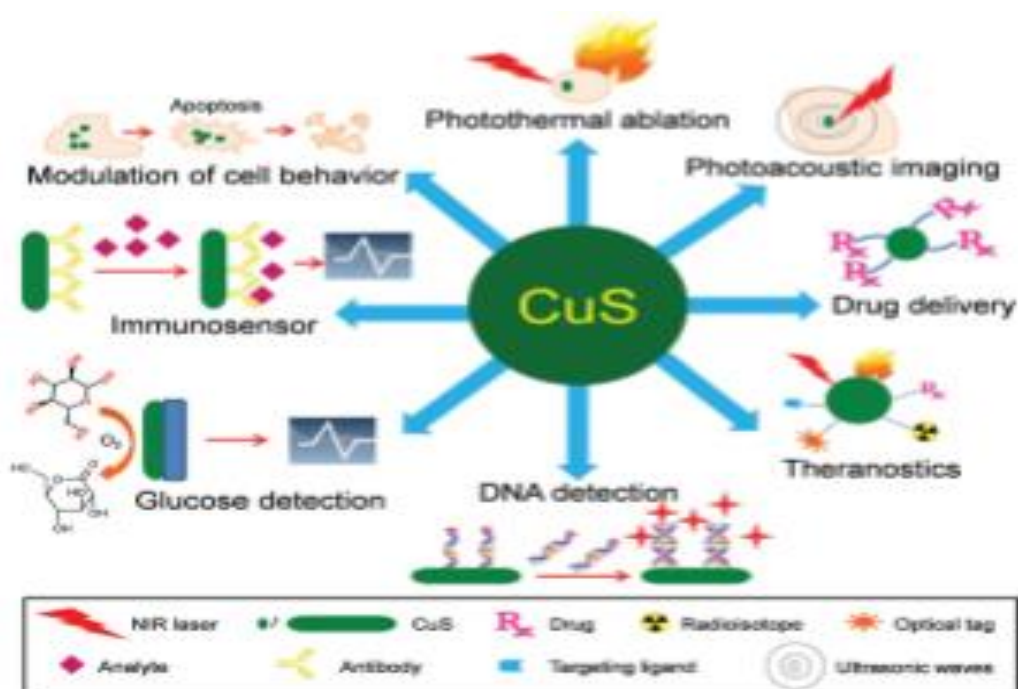
Fig. 1.4: Applications of CuS

Copper sulfide nanoparticles are also used as a catalyst. As catalyst they are used in the degradation of MB (Methyl Blue) in the presence of hydrogen peroxide in dark. After performing the experiment when the absorbance of MB was measured by UV- Vis then it was found that the absorbance was decreased. This decrease in absorbance confirmed the degradation of MB. This shows the catalytic effect of copper sulfide in the presence of H_2O_2 .The band gaps 2.08, 2.06, 2.16, and 1.88 eV are well suited for use as catalyst (Fig. 1.5).
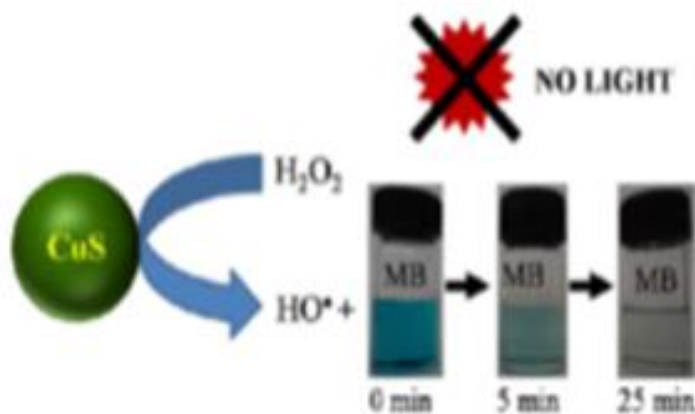
Fig.1.5: Degradation of MB using CuS

In another study, it was found that UV-Vis absorption intensity of eosin was decreased with time using CuS nanotubes. This shows that copper sulfide has photo catalytic properties and also exhibits good photo degradation efficiency. This was proved by two facts:

- Due to UV light absorption electron hole pair was created on the surface of copper sulfide nanotubes. This electron hole pair was responsible for the oxidation and reduction of eosin solution.

- Due to excellent suspending property of copper sulfide nanotubes the flocculent products were suspended in water for 15 days. As a result sufficiently good contact was established between copper sulfide nanotubes and eosin and photo degradation efficiency was improved. Due to this photo degradation property copper sulfide nanotubes are used for eliminating environmental pollution [51].

Copper sulfide nanoparticles are also used in photo acoustic imaging. In photo acoustic imaging laser light is absorbed by the molecules of the body like hemoglobin and melanin or exogenous contrast agents like copper sulfide. These molecules after absorbing light generate heat. This leads to thermo elastic expansion and ultrasound signals [52].

1.6. Photo catalysis

Photo catalysis is the acceleration of photoreaction in presence of some source of light. Photo catalytic activity depends upon the ability of the catalyst to generate electron hole pairs which generate free hydroxyl radical ($OH^{.}$) which then initiates
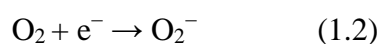
some secondary reactions. Photo catalytic degradation activity depends upon the adsorption activity of the pollutant molecules on the surface of the catalyst. More the adsorption of pollutant on the surface of the catalyst, more will be the degradation activity.
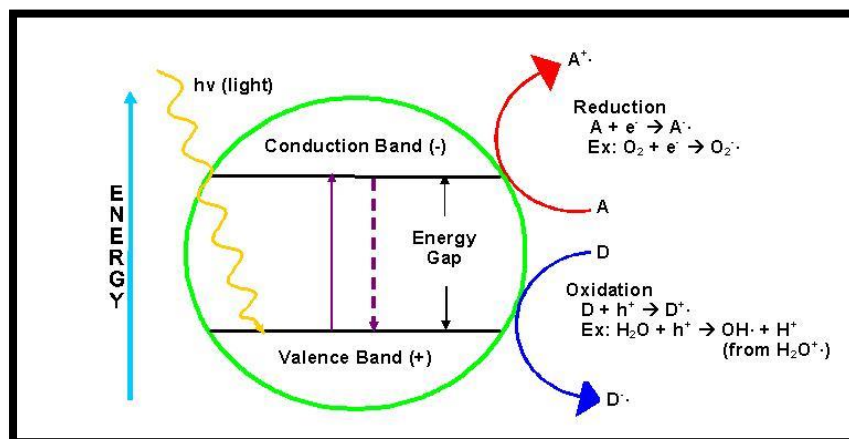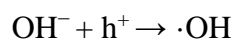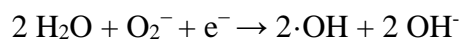

Fig.1.6: Photocatalysis

Here in this figure 1.6 it is seen that when a light (hυ) from a source falls on the catalyst surface, it excites electron from the valence band to the conduction band. Nanoparticles with band gap 2.2-3 eV are ideal for use as photocatalyst.

When a photon is made incident on the semiconductor, it results in the formation of electron hole pairs. These electron hole pairs are responsible for the formation of current, this is called photoconductivity. The conductivity of semiconductors depends on the number of electrons in the conduction band and number of holes in valence band. The energy of the photon should be greater than energy of band gap. The amount of current produced depends on the intensity of the incident light. This phenomena is used in photographic light meters. Photo conductivity is also the underlying principle of photovoltaic cell (solar cell). The electron hole recombination capacity of semiconductor increases with an increase in the number of holes and electrons. More the number of electrons and holes more will be the chances of recombination.

$$H_2O + h^+ \rightarrow \cdot OH + H^+ \quad (1.1)$$

$$O_2 + e^- \rightarrow O_2^- \quad (1.2)$$

$$2\ H_2O + O_2^- + e^- \rightarrow 2 \cdot OH + 2\ OH^-$$

$$OH^- + h^+ \rightarrow \cdot OH$$

Scheme 1: OH radical generation.

The OH· Radical produced (scheme 1) is responsible for the degradation of dyes [53] as shown in Fig. 1.7.
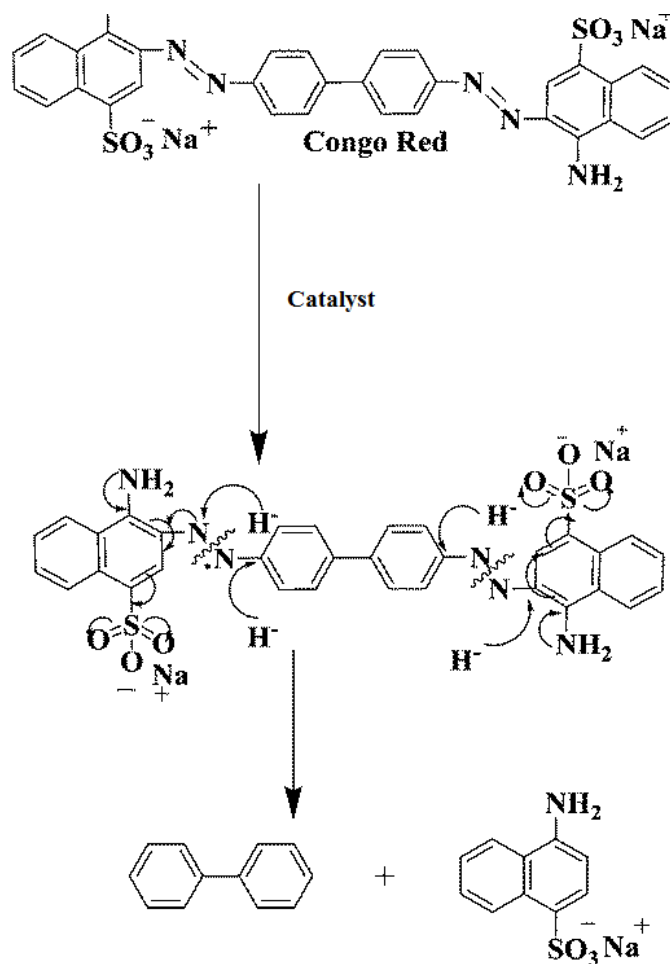

Fig. 1.7: Mechanism of degradation of Congo red [54]

REFERENCES

1. Bruus, H; Introduction to Nanotechnology, (2004)

2. Roco, M.C; Broader societal issues of nanotechnology, J. Nanopart. Res. 5 (2003) 181–189

3. Ramanathan, V; Crutzen, P. J; Kiehl, J.T; and Rosenfeld, D; Aerosols, Climate, and the Hydrological Cycle, Science. 294 (2001) 2119–2124

4. The Royal Society, & the Royal Academy of Engineering. Nanoscience and nanotechnologies: opportunities and uncertainties, (2004)

5. Bell, A; The impact of nanoscience on heterogeneous catalysis, Science. 299 (2003) 1688–1691

6. Edwards, P; and Thomas, J; Gold in a metallic divided state - from Faraday to present-day nanoscience, Angewandte Chemie International Edition. 46 (2007) 5480–5486

7. Tan, M; Wang, G; Hai, X; Ye, Z; and Yuan, J; Development of functionalized fluorescent europium nanoparticles for bio labeling and time-resolved fluorometric applications, J. Mater. Chem. 14 (2004) 2896-2901

8. Sinani, V.A; Koktysh, D.S; Yun, B.G; Matts, R.L; Pappas, T.C; Motamedi, M; Thomas, S.N; and Kotov, N.A; Collagen coating promotes biocompatibility of semiconductor nanoparticles in stratified LBL films, Nano Lett. 3 (2003) 1177-1182

9. Roy, I; Ohulchanskyy, T.Y; Pudavar, H.E; Bergey, E.J; Oseroff, A.R; Morgan, J; Dougherty, T.J; Prasad, P.N; Ceramic-based nanoparticles entrapping water-insoluble photosensitizing anticancer drugs: a novel drug-carrier system for photodynamic therapy, J. Am. Chem. Soc. 125 (2003) 7860-7865

10. Feynman, R.P; There's Plenty of Room at the Bottom. Engineering and Science, Caltech Engineering and Science. 23, (1960) 22-36

11. Kamazani, M.M; Niasari, M.S; Preparation of Stoichiometric Cu_2S Nanoparticles by Ultrasonic Method, Proc. NAP 2. 2 (2013) 1862-2304

12. Pua, F; Chia, C.H; Zakaria, S; Liew, T.K; Yarmo, M.A; & Huang, N.M; Preparation of Transition Metal Sulfide Nanoparticles via Hydrothermal Route, Sains Malays. 39 (2010) 243–248

13. Chen, Q; Shen, X; Gao, H; Formation of nanoparticles in water-in-oil micro emulsions controlled by the yield of hydrated electron: The controlled reduction of Cu^{+2}, J. Colloid. Interf. Sci. 308 (2007) 491–499

14. Shen, G; DiChen; Tang, K; Liu, X; Huang, L; and Qian,Y; General synthesis of metal sulfides nanocrystallines via a simple polyol route, J. Solid State Chem. 173 (2003) 232–235

15. Kuru, H.K; Coombes, M.J; Neethling, J.H; Westraadt, J.E; Fabrication of Cu_2S Nano needles by self-assembly of nanoparticles via simple wet chemical route , J. Alloy Compd. 589 (2014) 67–75

16. Lind, C; Gates, S.D; Pedoussaut, N.M; and Baiz, T.I; Novel Materials through Non-Hydrolytic Sol-Gel Processing: Negative Thermal Expansion Oxides and Beyond, Materials. 2010, 3, 2567-2587

17. Demazeau, G; Solvothermal Processes: Definition, Key Factors Governing the Involved Chemical Reactions and New Trends, Review. (2010) 999-1006

18. Pradhan, N; Katz, B; and Efrima, S; Synthesis of High-Quality Metal Sulfide Nanoparticles from Alkyl Xanthate Single Precursors in Alkyl amine Solvents, J. Phys. Chem. 107 (2003) 13843-13854

19. Jung, Y.K; Kim, J; and Lee, J.K; Thermal Decomposition Mechanism of Single-Molecule Precursors Forming Metal Sulfide Nanoparticles, J. Am. Chem. Soc. 132 (2010) 178–184

20. Hwang, J.H; Edward, D.D; Kammler, D.R; Masson, T.O; Point defects and electrical properties of Sn-doped In-based transparent conducting oxides, Solid State Ionics. 129 (2000) 135–144

21. Suja,R; Geetha, D; .and Ramesh,P; Preparation and characterization of CuS Nanomaterials by Solvothermal process, International Journal of Scientific & Engineering Research. 4 (2013) 2229-5518

22. Liu, Z.P; Liang, J.B; Qian, Y.T et al. A facile chemical route to semiconductor metal sulfide nanocrystals superlattice, Chem Commun. 24 (2004) 2724-2725

23. Gorai, S; Ganguli, D; and Chaudhuri, S; Synthesis of Copper Sulfides of Varying Morphologies and Stoichiometries Controlled by Chelating and Non chelating Solvents in a Solvothermal Process, J. Cryst. Growth. 5 (2005) 875-877

24. Plante, I. J. L; Zeid, T.W; Yang, P; and Mokari, T; Synthesis of metal sulfide nanomaterials via thermal decomposition of single-source precursors, J. Mater. Chem. 20 (2010) 6612–6617

25. Bera, P; Seok, S.II; Nanocrystallines copper sulfide of varying morphologies and stoichiometries in a low temperature Solvothermal process using a new single-source molecular precursor, Solid State Sci. 14 (2012) 1126-1132

26. Iwaski, F; Iwaski, H; Historical review of quartz crystal growth, J. Cryst. Growth. 237-239 (2002) 820-827

27. Oka, K; Shubata, H; Kashiwaya, S; Crystal growth of ZnO, J. of Cryst. Growth. 237-239 (2002) 509-513

28. Ohshima, E; Ogino, H; Niikura, I; Maeda, K; Sato ,M; Ito, M; Fukuda ,T; Growth of the 2-in-size Bulk ZnO single Crystals by the Hydrothermal Method, J. Cryst. Growth. 260 (2004) 166

29. Pradhan,N; Efrima,S; Single-precursor, one-pot versatile synthesis under near ambient conditions of tunable, single and dual band fluorescing metal sulfide nanoparticles, J. Am. Chem. Soc. 125 (2003) 2050

30. Itoh, K; Kuzuya, T; and Sumiyama, K; Morphology and Composition-Controls of Cu_xS Nanocrystals Using Alkyl-Amine Ligands, Mater. Trans. 47 (2006) 1953-1956

31. Ajibade, P.A; Onwudiwe, D.C; Moloto, M.J; Synthesis of hexadecylamine capped nanoparticles using group 12 complexes of N-alkyl-N-phenyl dithiocarbamate as single-source precursors, Polyhedron. 30 (2011) 246–25

32. Barreca, D; Gasparotto, A; Maragno, C; Seraglia, R; Tondello, E; Venzo, A; and Krishnan, V; Cadmium O-alkylxanthates as CVD precursors of CdS: a chemical characterization, Appl. Organomet. Chem. 19 (2005) 59–67

33. Ritch, J. S; Chivers, T; Ahmad, K; Afzaal, M; and O'Brien, P; Synthesis, structures, and multinuclear NMR spectra of tin (II) and lead (II) complexes of tellurium-containing imidodiphosphinate ligands: preparation of two morphologies of phase-pure PbTe from a single-source precursor, Inorg. Chem. 49 (2010) 1198–2005

34. Duan, T; Lou, W; Wang, X; and Xue, Q; Size-controlled synthesis of orderly organized cube-shaped lead sulfide nanocrystals via a Solvothermal single-source precursor method, Physicochemical Engineering Aspects. 310 (2007) 86–93

35. Plante, I. J. L; Zeid, T.W; Yang, P; and Mokari, T; Synthesis of metal sulfide Nano materials via thermal decomposition of single-source precursors, J. Mater. Chem. 20 (2010) 6612-6617

36. Green, M; Prince, P; Gardener, M; Steel, J; Mercury (II) *N,N*-methyl phenyl ethyl dithiocarbamate and its use as a precursor for the room temperature solution deposition of β-HgS thin film, Adv.Master. 16 (2004) 994

37. Brien, O.P; Zhang, X; Motevalli, M; Synthesis of PbS nanocrystals using a novel single molecule precursor approach: X-ray single crystal structure of Pb (S$_2$CNEtPr^i) $_2$, J. Mater. Chem. 7 (1997) 1011

38. Ngo, S.C; Banger, K.K; Delarosa, M.J; Toscano, P.J; Welch, J.T; Thermal and structural characterization of a series of homoleptic Cu (II) dialkyldithiocarbamates complexes: bigger is only marginally better for potential MOCVD performance, Polyhedron. 22 (2002) 1575–1583

39. Siddiqi, K.S; Nami, S.A.A; Lutfullah; Chebude, Y; Synthesis, Characterization and Thermal Studies of Bipyridine Metal Complexes Containing Different Substituted Dithiocarbamates Synthesis and Reactivity in Inorganic, Metal-Organic and Nano-Metal Chemistry. 35 (2005) 445–451

40. Plante, I.J.L; Zeid, T.W; Yang, P; and Taleb; Synthesis of metal sulfide nanomaterials via thermal decomposition of single-source precursors, J.Mater.Chem.20 (2010) 6612–6617

41. Sharma, A.K; Thermal Behavior of metal dithiocarbamates, Thermochim. Acta. 104 (1986) 339-372

42. Nomura, R; Kanaya, K; Matsuda, M; Preparation of Copper Sulfide Powders and Thin Films by Thermal Decomposition of Copper Dithiocarbamate Complexes, Ind. Eng. Chem. Res. 28 (1989) 877-880

43. Liu, Z; Xu, D; Liang, J; Shen, J; Zhang, S; Qian, Y; Growth of Cu$_2$S ultrathin nanowires in a binary surfactant solvent, J. Phys. Chem. B. 109 (2005) 10699-704

44. Basu, M; Sinha, A.K; Pradhan, M; Sarkar, S; Negishi, Y; Pal, G; Pal, T; Evolution of hierarchical hexagonal stacked plates of CuS from liquid-liquid interface and its photocatalytic application for oxidative degradation of different dyes under indoor lighting, Environ. Sci. Technol. 44 (2010) 6313-8

45. Grozdanov, I; Electroless chemical deposition technique for Cu$_2$O thin films, 19 (1994) 281–285

46. Du, Y; Yin, Z; Zhu, J; Huang, X; Wu, X. J; Zeng, Z, Yan, Q; & Zhang, H; A general method for the large-scales synthesis of uniform ultrathin metal sulphide nanocrystals, Nat. Commun. 3 (2012) 1177

47. Chen, X; Zhang, X.E; Chai, Y.Q; Hu, W.P; Zhang, Z. P; Zhang, X. M; Cass, A. E; DNA optical sensor: A rapid method for the detection of DNA hybridization, Biosens. Bioelectron. 13 (1998) 451-8

48. Lee ,H; Yoon, S.W; Kim, E.J; Park, J; In situ growth of Copper sulfide nanocrystals on multiwalled carbon nanotubes and their applications as novel solar cells and amperometric glucose sensor materials, Nano Lett. 7 (2007) 778

49. Wu, Y; Wadia, C; Ma, W; Sadtler, B; and Alivisatos, A.P; Synthesis and Photovoltaic Application of Copper (I) Sulfide Nanocrystals, Nano Lett. 8 (2008) 2551-2555

50. Liu, Z; Xu, D; Liang, J; Shen, J; Zhang, S; Qian, Y; Growth of Cu_2S ultrathin nanowires in a binary surfactant solvent, J. Phys. Chem. B. 109 (2005) 10699-704

51. Wang, X.Y; Fang, Z; Lin, X; Copper sulfide nanotubes: facile, large-scale synthesis, and application in photo degradation, J. Nanopart. Res. 11 (2009) 731–736

52. Wang, L.V; Hu, S; Photoacoustic tomography: in vivo imaging from organelles to organs, Science. 335 (2012) 1458-1462

53. Soltania, N; Saiona, E; Yunusa, W. M. M; Erfania, M; Navaserya, N; Bahmanrokha, G; Rezaeeb, K; Enhancement of visible light photo catalytic activity of ZnS and CdS nanoparticles based on organic and inorganic coating, Appl. Surf. Sci. 290 (2014) 440-447

54. Rajesh, R; Kumar, S.S; and Venkatesan, R; Efficient degradation of azo dyes using Ag and Au nanoparticles stabilized on graphene oxide functionalized with PAMAM dendrimers, New J. Chem. 38 (2014) 1551

CHAPTER 2

EXPERIMENTAL

2.1 Chemicals

About precursors were used as received. $CuCl_2.2H_2O$ was purchased from Merck, NaOH from Fluka and substituted piperazine and piperidine were purchased from Sigma- Aldrich Company.

2.2 Solvents

All solvents used were of analytical grade. Methanol, chloroform and toluene were purchased from Dae Jung, DMSO from Riedel de Haen and DMF, DCM, acetone, ethylene diamine and octylamine were purchased from Sigma Aldrich.

2.3 Instrumentation

Sanyo electro thermal melting point apparatus was used to take the melting point of ligands and complexes. Nicolet 6700 Infra-red Spectrophotometer (Thermo scientific USA) was used to record the infra-red spectra of compounds and ligands. Shimadzu double beam spectrophotometer 1800 was used to take the UV-Vis spectra of nanoparticles. UV- Analyselampe SN: 500412 was used to provide UV source whose wavelength was 254 nm.

2.4 General procedure for the preparation of ligands

About 0.03 moles of substituted piperazine or piperidine were dissolved in methanol and NaOH dissolved in methanol was added. After 4 hours stirring, 0.03 moles of methanolic solution of CS_2 was added drop wise maintaining the temperature around $0^{\circ}C$. The temperature was maintained at $0^{\circ}C$ by using ice bath. The resulting solution was stirred for 8 hours and after that the solution was rotary evaporated to get corresponding salts of dithiocarbamate ligand.

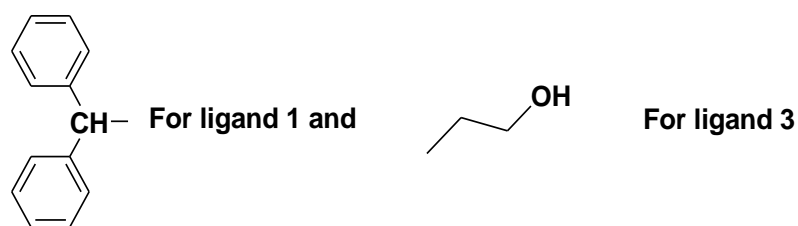## General scheme 1 for the preparation of ligands from piperazine derivatives is as follow

General scheme for preparation of ligand is as follows

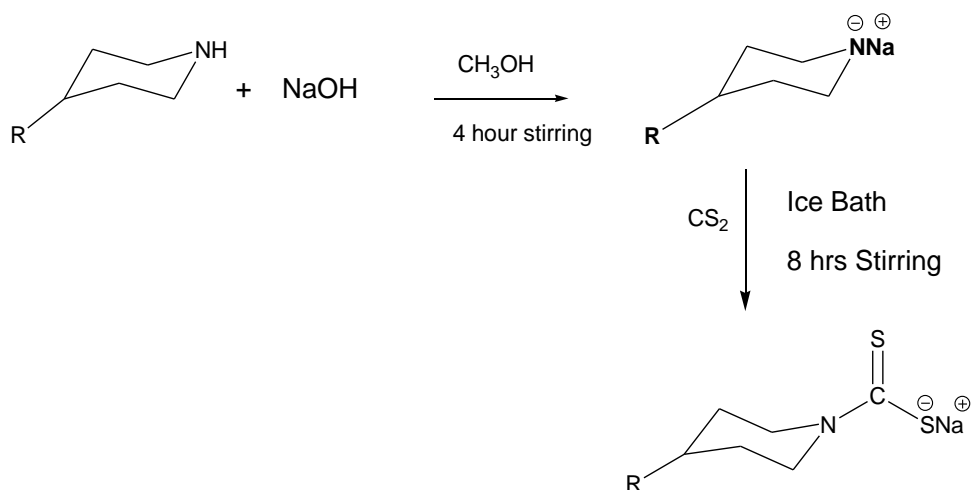Here R groups are

CH— **For ligand 1 and**
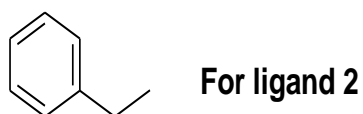
OH **For ligand 3**
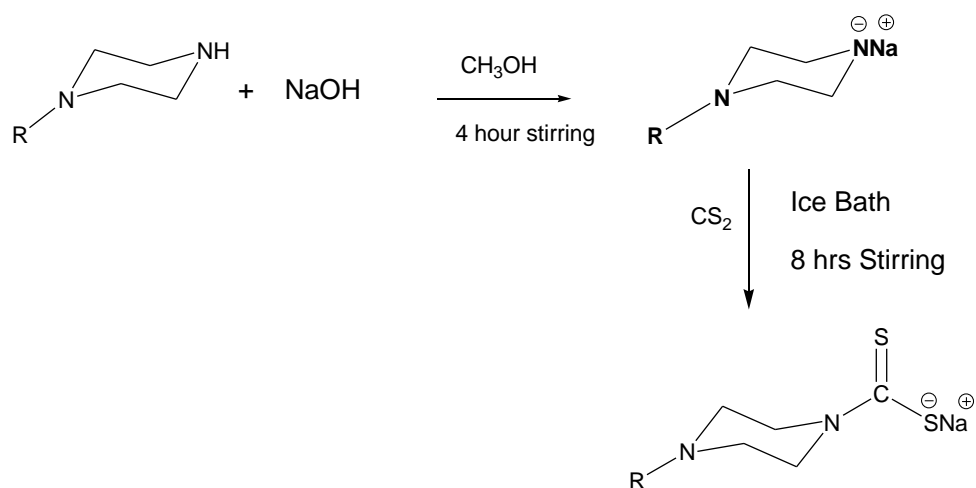
General scheme 2 for preparation of ligands from piperidine derivatives is as follows

Here R group is

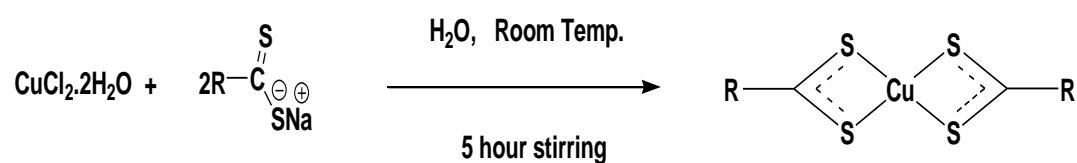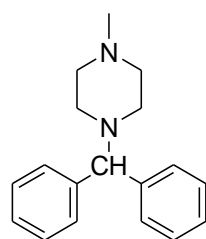**For ligand 2**

2.5 Synthesis of complexes

Procedure for the synthesis of complexes is
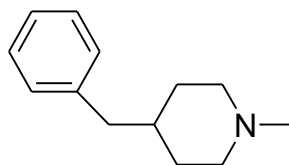
2.5.1 General procedure for synthesis of complexes

To aqueous solution of ligand (known amount), $CuCl_2.2H_2O$ (known amount) dissolved in distilled water was added drop wise. Metal salt solution to ligand solution ratio was taken 1:2. Brown colored precipitates were obtained which were then filtered, washed and dried.
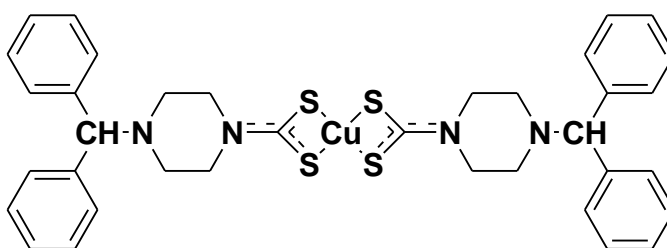

Here R are

| For ligand 1 | ligand 2 | ligand 3 |
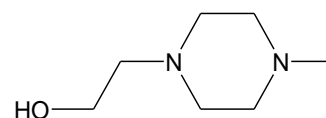
Scheme 3 for synthesis of complexes

2.5.1.1 Complex 1

1.427 mmoles (0.5g) Sodium 4-benzhydrylpiperazine-1-carbodithioate and 0.732mmoles (0.1216 g $CuCl_2$. $2H_2O$) were taken. The yield obtained from this was 0.47g (91.7%). Its M.P is 262^0C. The complex was recrystallized from chloroform.

2.5.1.2 Complex 2

1.829 mmole (0.5g Sodium 4-benzylpiperidine-1-carbodithioate) and 0.915mmole (0.156 g) $CuCl_2$. $2H_2O$ were taken. Yield obtained from this reaction was 0.343 g (68.6 %). Its M.P is 250^0C. The structure of the complex is
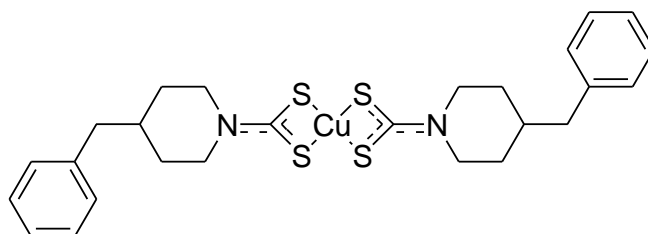
2.5.1.3 Complex 3

0.5g (2.19 mmole) of sodium 4-(2-hydroxyethyl) piperazine-1-carbodithioate and 0.186 g (1.09 mmole) $CuCl_2$. $2H_2O$ were taken. Yield obtained from this reaction was 0.448 g (86.4%). Its M.P is from 245-247^{0}C. The complex was recrystallized from DCM. [1] .The structure of the complex is
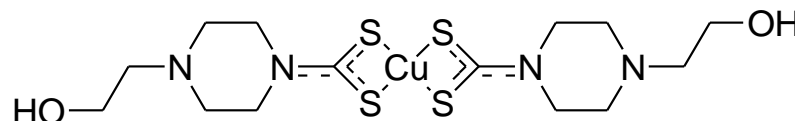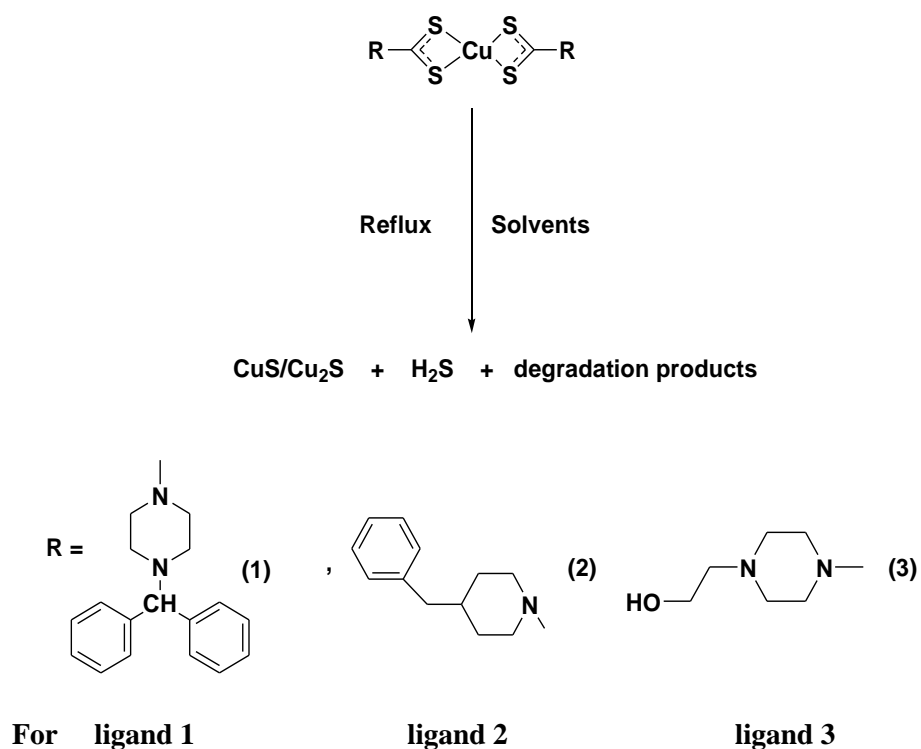

2.6 Synthesis of nanoparticles

0.7g each copper complex was added to two neck flask containing 12-14 mL of ethylenediamine/octylamine. The temperature was allowed to rise up to $120^{\circ}C/140^{\circ}C$ with continuous stirring. The black colored copper sulfide (Cu_2S/CuS in ethylenediamine [2] and pure CuS in octylamine) nanoparticles (NPs) were obtained. The H_2S liberated was allowed to escape through a bent tube into a test tube containing lead nitrate solution; black colored PbS nanoparticles were formed immediately (confirmed by EDS). The reaction mixture was stirred at this temperature for about one hour. Copper sulfide NPs was filtered and washed with methanol. The sample was characterized by UV, XRD, TEM and EDS.

COPPER SULFIDE NANOPARTICLES

Scheme: Solvothermal synthesis of copper sulfide nanoparticles.

Table.1: Synthesis of CuS/Cu$_2$S from scheme 1

Sr. No	Reactants	Reaction temperature (^{0}C)	Composition of Nanoparticles	Sample codes
1.	Complex 1+ EN	120	CuS/Cu$_2$S	NP.1
2.	Complex 2+ EN	120	CuS/Cu$_2$S	NP.2
3.	Complex 3+ EN	120	CuS/Cu$_2$S	NP.3

Table.2: Synthesis of CuS from scheme 2

Sr. No	Reactants	Reaction temperature (^{0}C)	Composition of Nanoparticles	Sample codes
1.	Complex 1+ OA	140	CuS	NP.4
2.	Complex 2+ OA	140	CuS	NP.5
3.	Complex 3+ OA	140	CuS	NP.6

2.7 XRD

XRD characterization was done in order to investigate the formation of copper sulfide nanoparticles. X Ray Powder Diffraction was performed using PANalytical X´Pert[3] Pro Powder instrument with Cu kα radiation (λ = 1.54178 A^0). 2 theta value was maintained from 10 to 80.

2.8 TEM

The high resolution transmission electron microscope (HRTEM) images of the nanoparticles were obtained at accelerating voltage of 200 kV using copper mesh.

2.9 Dye degradation studies

Commercially available Congo red dye $C_{32}H_{22}N_6Na_2O_6S_2$ was purchased from local supplier. 100 ppm of dye solution was prepared by dissolving about 0.05g of Congo red dye in 500mL distilled water. Congo red dye shows three peaks.
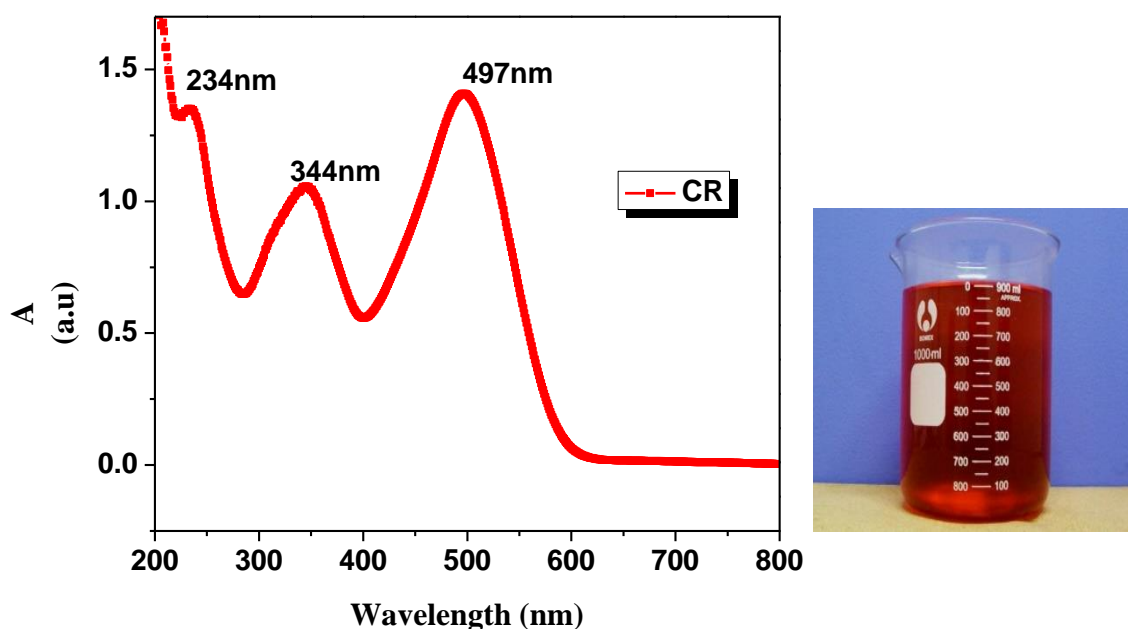

Fig. 2.1. : UV Vis spectra of Congo dye

The peak at 497nm is due to -N=N- group. This is a chromophore. The peaks at 234nm and 344 nm are due to benzene and naphthalene groups respectively.

COPPER SULFIDE NANOPARTICLES

Photo catalytic experiments were performed in Pyrex flask (100mL). UV-Analyselampe SN: 500412 was used to provide UV source whose wavelength was adjusted at 254 nm. A 100mL of 100ppm Congo red solution was mixed with about 0.05g CuS nanoparticles and was put under UV lamp. The sample was collected after every 10 min and the concentration of CR was found by Shimadzu double beam spectrophotometer 1800 scanning from 200nm to 800nm. The wavelength at the maximum absorbance (497nm) was monitored after every 10 min interval. A calibration plot was plotted between absorbance and concentration. This calibration graph was based on Beer Lambert law. The same experiment was performed under visible light and in dark in order to observe the economic utility of these nanoparticles.

Degradation rate was calculated using following equation.

$$\% \text{ degradation efficiency} \quad = \quad \frac{C_0 - C_i}{C_0} \times 100$$

Where

C_0 is the initial concentration of Congo red

C_i is the concentration of Congo red at certain reaction time t (min)

Photocatalytic reaction kinetics on photo catalyst can be expressed by Langmuir-Hinshelwood model. The reaction rate can be expressed as

$$\ln C_i/C_o = - k_{app} \, t$$

Where k_{app} is the apparent pseudo-first-order reaction rate constant and t is the reaction time. A plot of $\ln (C_i/C_0)$ versus t will yield a slope of $(-k_{app})$.

REFERENCES

1. Ali, R.F; Spectroscopic and X-Ray Single Crystal Characterization of New Bioactive Sulfur Bridged Homobimetallic Copper (II) Dithiocarbamates, 2014

2. Gorai, S; Ganguli, D; and Chaudhuri, S; Synthesis of Copper Sulfides of Varying Morphologies and Stoichiometries Controlled by Chelating and Non chelating Solvents in a Solvothermal Process, Cryst. Growth Des. 5 (2005) 875-877.

CHAPTER 3

RESULTS AND DISCUSSIONS

3.1 Physical data

Physical data of ligands and complexes are given in Table 3.1 & 3.2. All the three ligands are pale yellow in color. They have sharp melting points ranging from 106-232 ^{0}C. They are soluble in solvents like H_2O, CH_3OH whereas copper complexes are soluble in variety of solvents like $CHCl_3$, DCM, DMSO and C_2H_5OH. All the complexes are brown in color and they are crystalline in nature. Their melting point range from 240-264 ^{0}C.

Table 3.1: Physical data of dithiocarbamate ligands

Sr. no	Molecular formula	Physical state	Melting point ^{0}C	Solubility
1	$NaC_{18}H_{19}N_2S_2$(L1)	Pale yellow solid	106-109	H_2O, CH_3OH
2	$NaC_{12}H_{16}NS_2$(L2)	Pale yellow solid	126-128	H_2O, CH_3OH
3	$NaC_7H_{13}N_2OS_2$(L3)	Pale yellow solid	230-232	H_2O, CH_3OH

Table 3.2: Physical data of dithiocarbamate complexes

Sr. no	Molecular formula	Physical state	Melting point ^{0}C	Solubility
1	$C_{36}H_{38}N_4S_4Cu$ (1)	Brown Crystalline Solid	262-264	DCM, $CHCl_3$, DMSO
2	$C_{24}H_{32}N_2S_4Cu$ (2)	Brown Crystalline Solid	240-242	DCM, $CHCl_3$, DMSO
3	$C_{14}H_{26}N_4O_2S_4Cu$ (3)	Brown Crystalline Solid	245-247	Toluene, DMF, DMSO

3.2 FT-IR Spectroscopy

There are some important peaks of dithiocarbamate and their complexes having structural significance. Usually the range of IR bands of dithiocarbamate ligands and their complexes is in the range of 1495-1412 cm^{-1} and 995-911 cm^{-1}. This range of 1495-1412 cm^{-1} is because of C-N bond stretching of thioureide group. The value fall between C=N (1680-1640 cm^{-1}) and C-N (1350-1250 cm^{-1}) bonds, thus signify partial double character. In metal complexes, C=N is shifted to high value of about 10-45 cm^{-1} thus indicate the bidentate bonding mode of dithiocarbamate ligand through S, S atoms.

Another important peak is in the range of 995-911 cm^{-1} due to C-S bond. If there is only one peak in above mentioned region then it will show the bidentate mode of bonding of the ligand. If the peak split in the above region and the difference in the peak is by 20 cm^{-1}, then it will indicate the monodentate mode of bonding of the ligand.

Another peak (Cu-S) that confirms the formation of the metal ligand complex is in far IR region. The peak for Cu-S bond in the range of 370-360 cm^{-1} confirms the formation of complex. This peak is. These peaks are absent in ligand and are only present in complexes [1]. These IR peaks are mentioned in table 3.3.

Table 3.3: Important FT-IR bands of ligands and their copper complexes

Sr. no	Compounds	υC-N (cm^{-1})	υC-S (cm^{-1})	υ Cu-S(cm^{-1})
1	$NaC_{18}H_{19}N_2S_2$(L-1)	1451	923	-
2	$C_{36}H_{38}N_4S_4Cu$ (1)	1489	968	360
3	$NaC_{12}H_{16}NS_2$ (L-2)	1425	980	-
4	$C_{24}H_{32}N_2S_4Cu$ (2)	1465	995	355
5	$NaC_7H_{13}N_2OS_2$ (L-3)	1415	978	-
6	$C_{14}H_{26}N_4O_2S_4Cu$ (3)	1495	996	358

3.3 UV-Visible Spectroscopy

3.3.1 Characterization of Cu_2S/CuS nanoparticles prepared via ethylenediamine

The UV-Visible spectrum of Cu_2S/CuS was recorded by dispersing NP.1, NP.2 and NP.3 nanoparticles in ethanol by sonication. The peaks at 542 nm and 566 nm (Fig. 3.1) show a blue shift from the bulk value of 1032 nm. This can be attributed to an increase in the band gap upon decrease in size of nanoparticles The Cu_2S NPs along with CuS NPs were formed due to the reducing nature of ethylenediamine [2]. The values obtained are comparable with the literature value [3]. The UV data shows that NP.1 and NP.2 are smaller in size than NP.3. The band gap calculated by Planck equation for 542nm was found to be 2.28 eV and that for 566nm was found to be 2.19eV. This confirms the fact that band gap increases with decrease in size. Less the band gap more will be the wavelength.
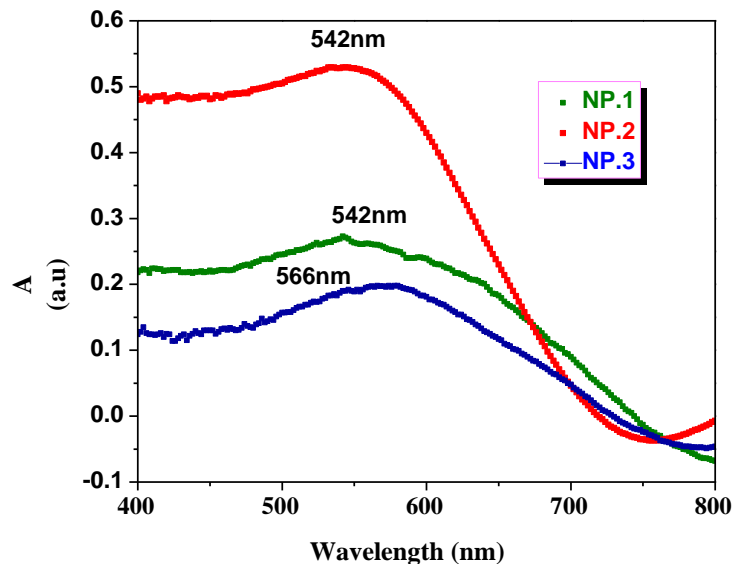
Fig. 3. 1. UV-Visible spectrum of Cu_2S/CuS nanoparticles

3.3.2 Characterization of CuS nanoparticles prepared via octylamine

The three NPs obtained via octylamine registered peaks at 404 nm, 388 nm and 406 nm (Fig 3.2). The higher blue shift in this case signified that the NPs obtained via octylamine are smaller in size than formed through ethylenediamine. Moreover, the size is comparable with already reported NPs of the same kind [4]. NP.5 has more blue shift in value which shows that it has smaller size as compared to NP.4 and NP.6. The band gap calculated for 404nm was found to be 3.06eV, for 388 to be 3.19eVand for 406nm

was 3.05eV. This confirms the fact that band gap increases with decrease in size. Less the band gap more will be the wavelength.

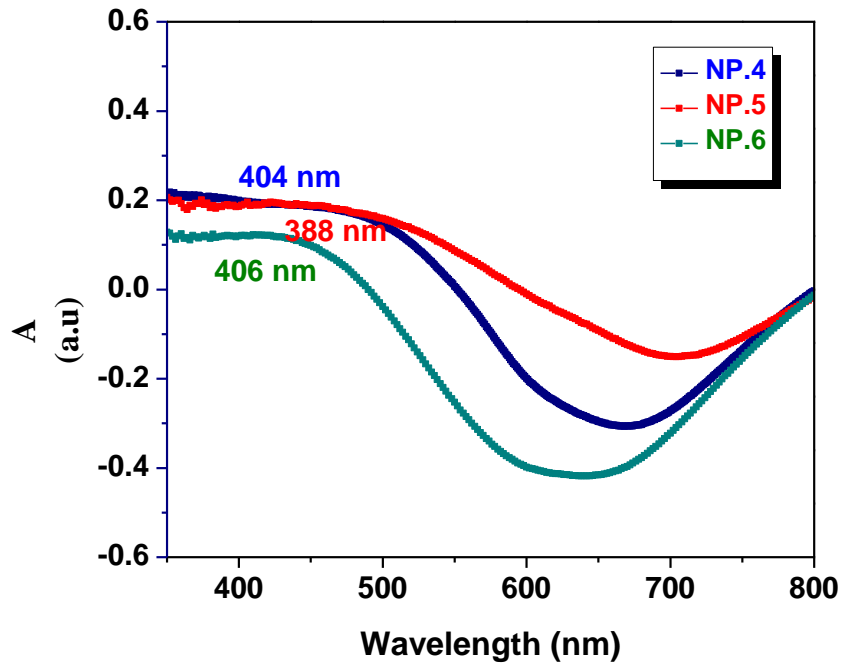**Fig 3.2. UV visible spectrum of CuS nanoparticles**

3.4 XRD Studies

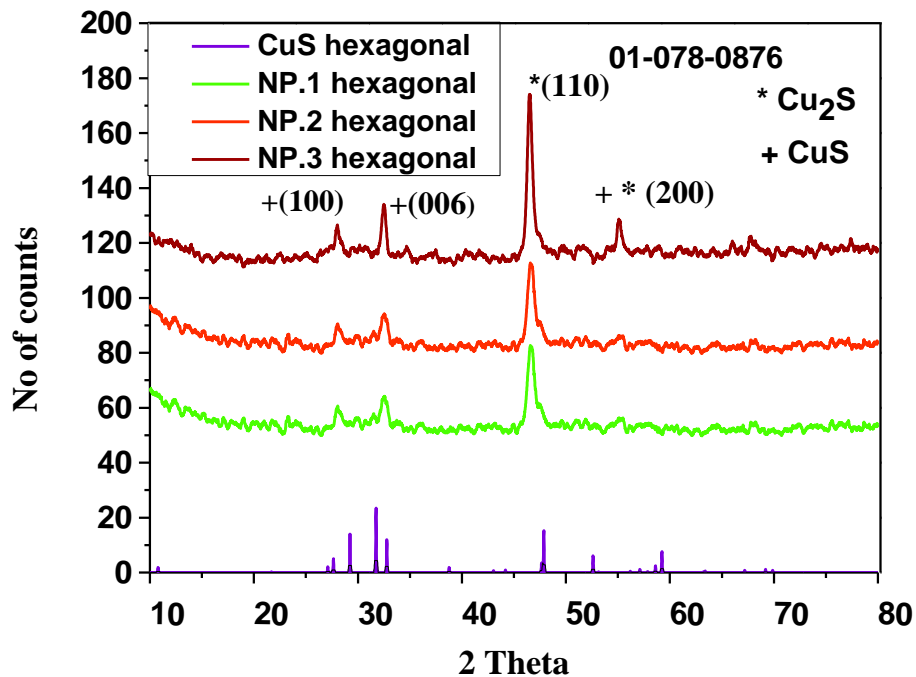## 3.4.1 XRD of Cu_2S/CuS nanoparticles prepared via ethylenediamine

Fig. 3.3: XRD of CuS/Cu_2S nanoparticles

The XRD spectra of black colored copper sulfide NPs showed in fig. 3.3 explained the formation of a mixed phase copper sulfide nanoparticles.

The NP.1 shows 2θ values at 27.97, 32.64 and 46.59. NP.2 shows 2θ values at 28.14, 32.64, 46.59 and 55.10 and NP.3 shows 2θ values at 27.71, 32.50, 46.51 and 55.11 (3.3) as shown in fig. 3.3. The peaks at 2θ values of 27.97, 27.71, 28.14, 32.64, 32.50, 55.10 and 55.11 also marked with asterisk (*) match with CuS [5]. On the other hand the 2θ values at 46.59, 46.51 and 55.11 marked with (+) sign match with Cu_2S. All of the NPs are hexagonal in shape. CuS nanoparticles are compared with JCPDS Card no. 01-078-0876 (Covelite) and Cu_2S nanoparticles are compared with JCPDS Card no. 00-026-1116 (chalcocite). The sharp and prominent peaks in XRD spectra confirmed the crystallinity of the NPs.

Table. 3.4 Summary of nanoparticles prepared from Cu precursor and EN

Sample Code	Formula	Crystal System
NP.1	CuS, Cu_2S	Hexagonal
NP.2	CuS, Cu_2S	Hexagonal
NP.3	CuS, Cu_2S	Hexagonal

3.4.2 XRD characterization of CuS NPs prepared via octylamine

The fig.3.4 shows 2θ values at 27.78, 29.46, 32.94, 48.23, 52.83 and 59.62 .NP.5 shows 2θ values at 27.78, 29.42, 32.47, 48.09, 52.83 and 59.49 and NP.6 shows 2θ values 27.78, 29.54, 31.98, 48.24, 53.06 and 59.66 as shown in Fig. 3.4. Here all the peaks matches with hexagonal CuS (Covelite). XRD is compared with JCPDS Card no. 00-006-0464 (Covelite). The sharp and prominent peaks in XRD spectra are in agreement with crystalline nature of NPs [6].The crystallite size was calculated using Debye Scherer formula

$$D = \frac{k\lambda}{\beta\cos\theta} \quad (3.1)$$

COPPER SULFIDE NANOPARTICLES

Where:

- D is the crystalline size

- K is the scherrer constant whose value is equal to 0.9

- λ is the X-ray wavelength. Its value is 1.54 angstrom

- β is the line broadening at half the maximum intensity (FWHM)

- θ is the Bragg angle
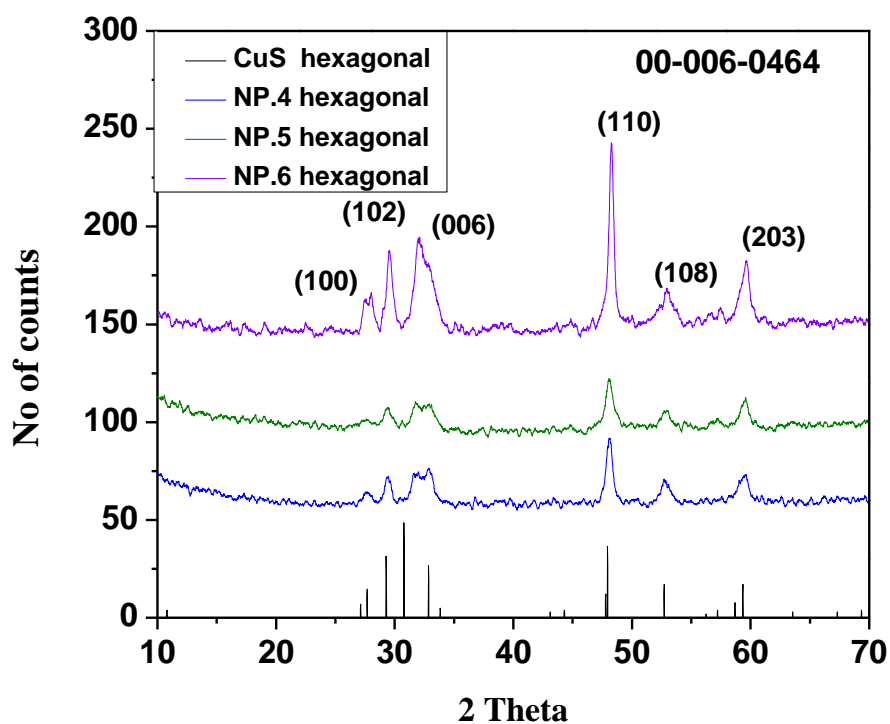
Fig. 3.4 XRD of CuS nanoparticles

Crystallite size of nanoparticles is given in table. 3.5

Table.3.5 summary of nanoparticles prepared from Cu precursor and OA

Sample Code	Formula	Crystallite Size	Crystal System
NP.4	CuS	7.9-17 nm	Hexagonal
NP.5	CuS	4.3-18 nm	Hexagonal
NP.6	CuS	9-42 nm	Hexagonal

3.5 TEM Characterization

3.5.1 Characterization of NP.2

The energy dispersive X-rays (EDX) of the sample NP.2 is shown in Fig. 3.5.

Element	Weight %	Atomic %
S	24.70	39.39
Cu	75.30	60.61
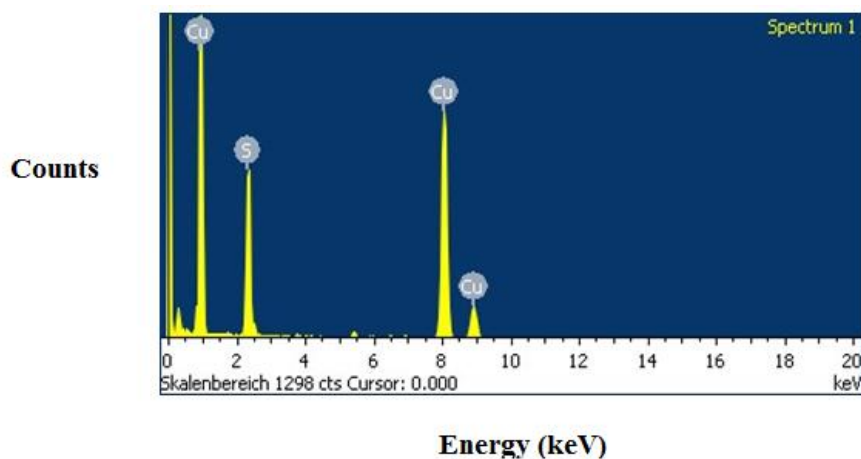
Fig. 3.5: EDX spectra of CuS

The EDX spectrum of NP.2 shows the presence of only Cu and sulfur. For Cu 60.61 % in which 20 % of Cu is from Cu mesh. Eliminating this Cu 20 % from total Cu suggests that Cu and S are present in 1:1 atomic ratio.

The TEM images with different magnifications are shown in Fig.3.6 (a-d). This CuS particles are hexagonal-shaped with particle size is in the range of 310-890 nm with an average diameter of 490 nm. The particle size histogram (Fig. 3.7) is deduced from TEM image for the CuS. The histogram is obtained after counting 41 particles cluster from the TEM image. The larger CuS particles can also be seen due to the agglomeration of smaller particles. The selected area electron diffraction (SAED) analysis on the CuS nanoparticles gave a clear diffraction pattern consisted of several rings thus confirming the crystalline nature of the NPs. The SAED analysis also confirmed the hexagonal structure observed in the TEM images of the CuS particles.

COPPER SULFIDE NANOPARTICLES

The hexagonal symmetry observed in the SAED pattern is consistent with Covelite structure of the CuS and chalcocite structure of Cu_2S. The pattern corresponds to hexagonal CuS in the space group *P6₃/mmc* (cell constants *a* = 3.796 A°, *c* = 16.380 A°; JCPDS 01-078-0876) [6]. The pattern of also corresponds to hexagonal Cu_2S in the space group *P6₃/mmc* (cell constants *a* = 3.9610 A°, *c* = 6.7220 A°; JCPDS 00-026-1116) [7]. The clear distribution of the SAED spots in Fig 3.8 indicates the single crystalline nature of the CuS nanoparticles. The HRTEM image of CuS nanoparticles (Fig. 3.9) shows clear visible lattice fringes and complements the SAED analysis, and provides the evidence of single crystal nature of the CuS nanoparticles Inter planar spacing 0.193nm, 0.306 nm and 0.188 nm matched with Cu_2S (Chalcocite) [7] and the Inter planar spacing 0.303 nm and 0.188 nm matched with CuS (Covelite). This shows the mixed phase of copper sulfide nanoparticles.
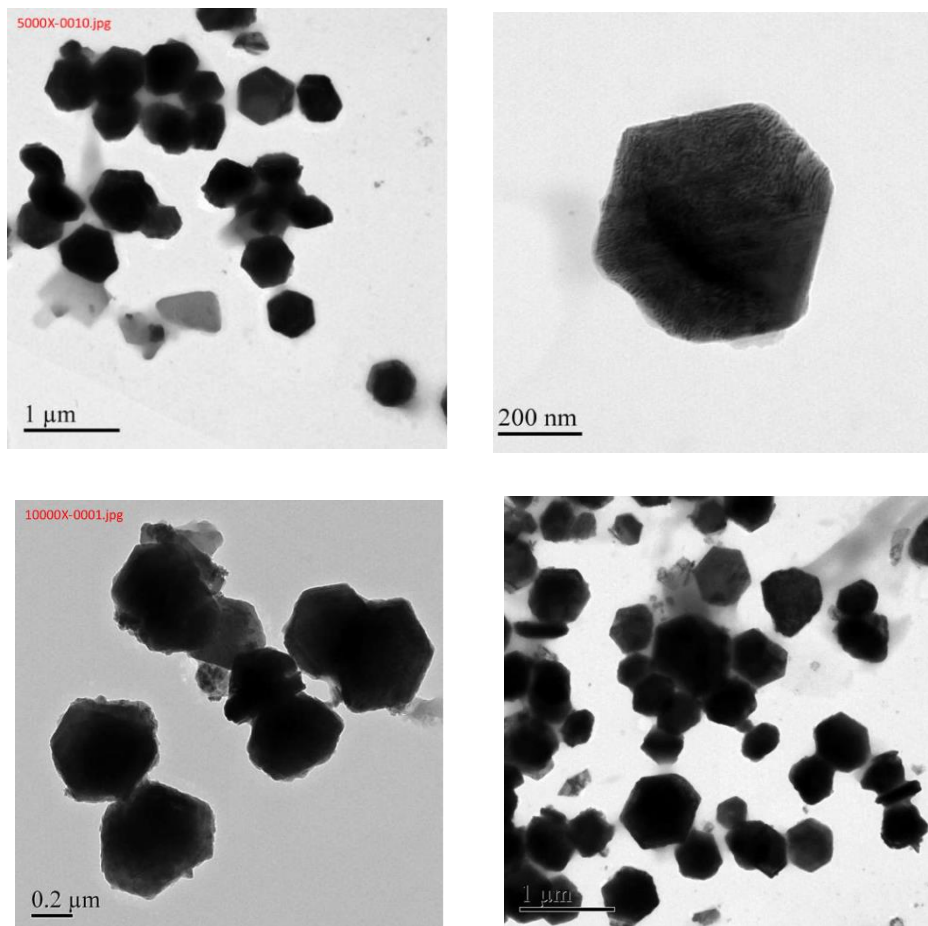
Fig. 3.6: TEM images of copper sulfide (a-d)
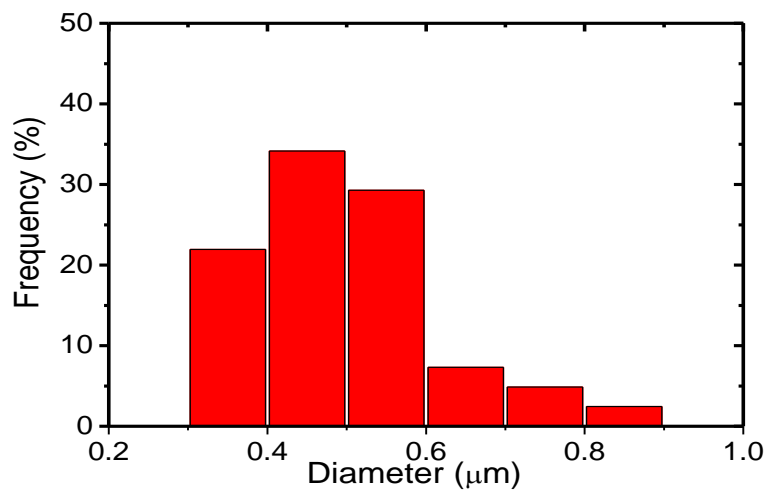
Fig. 3.7: Size Distribution Histogram of CuS/Cu₂S
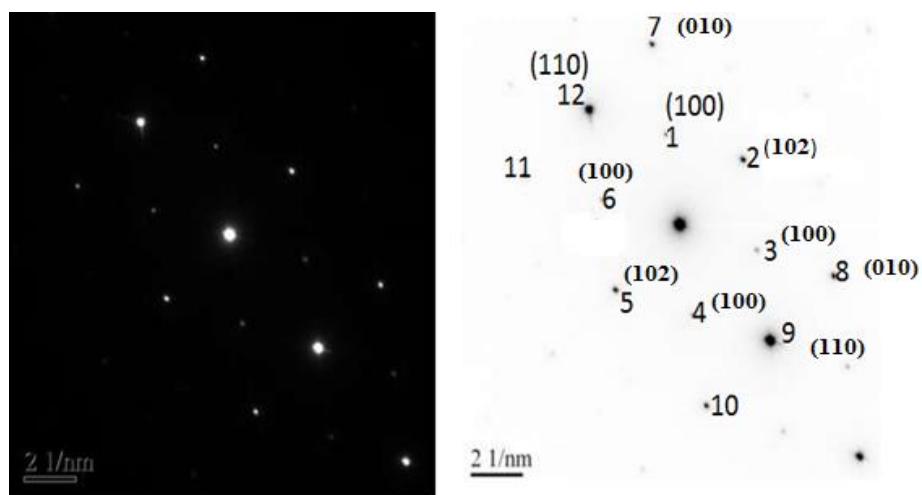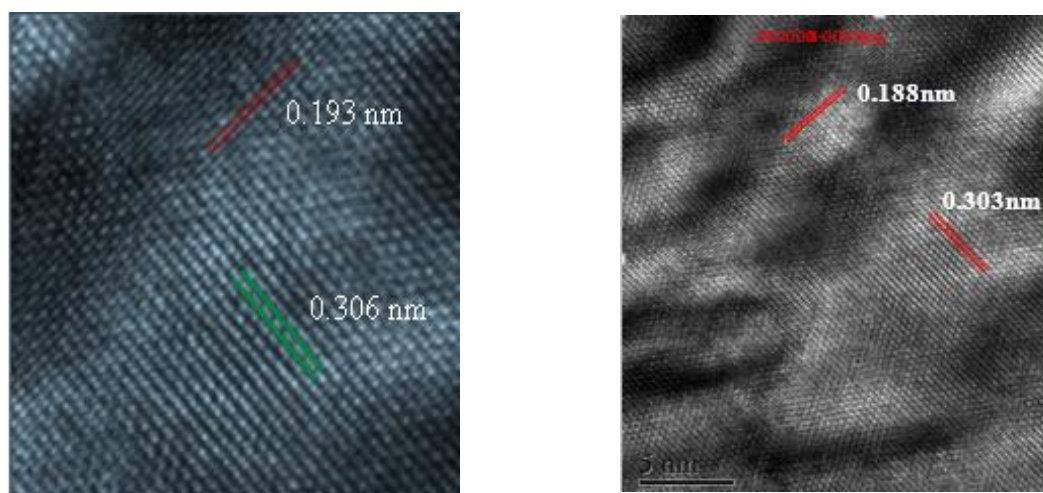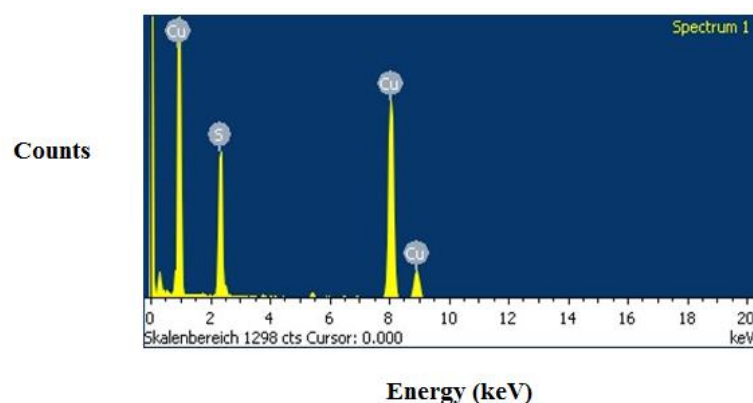

Fig. 3.8: SAED images of CuS/Cu₂S

Fig. 3.9: HRTEM image of CuS/Cu₂S

3.5.2 Characterization of NP.5

In EDX there is 20% contribution by Cu mesh. Eliminating this 20% Cu from total Cu sample suggest that Cu and S are in 1:1. The energy dispersive X-rays (EDX) of the sample NP.5 is shown in Fig. 3.10.

Element	Weight %	Atomic %
S	28.88	44.59
Cu	71.12	55.41

Fig. 3.10: EDS spectra of CuS.

The TEM images (Fig. 3.11) confirm the hexagonal shaped of CuS NPs with particle sizes in the range of 0.75-58.84 nm and with an average diameter of 35.39 nm. The particle size histogram (Fig. 3.12) is deduced from TEM image for the CuS. The histogram is obtained after counting 51 particles cluster from the TEM image. The larger CuS NPss can also be seen due to the agglomeration of smaller particles.
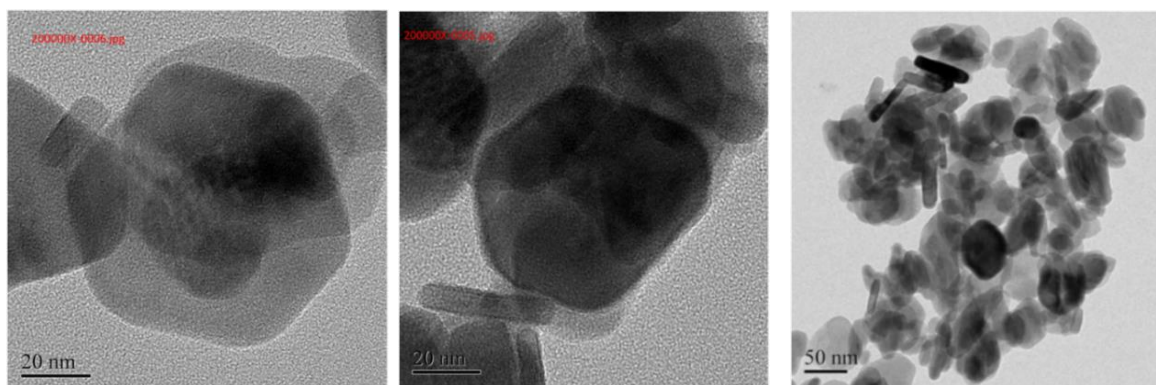

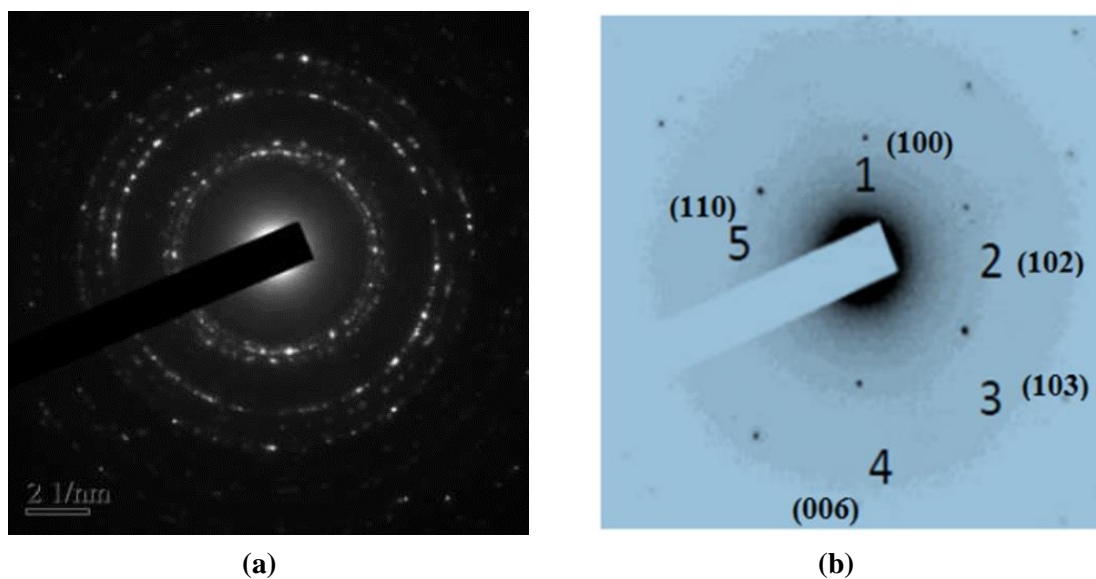Fig. 3.11: TEM images of copper sulfide (a-c)

COPPER SULFIDE NANOPARTICLES

The selected area electron diffraction (SAED) analysis on the CuS nanoparticles gave a clear diffraction pattern consisted of several rings thus confirming the crystallinity of NPs (Fig. 3.13). The SAED analysis also authenticated the hexagonal structure observed in the TEM images of the CuS particles.
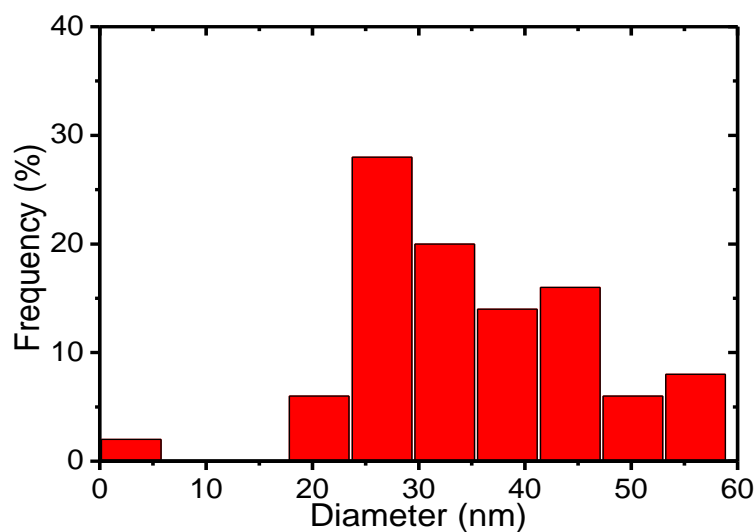
Fig. 3.12: Size Distribution Histogram of CuS

The hexagonal symmetry observed in the HRTEM pattern is consistent with Covelite structure of the CuS. The pattern corresponds to hexagonal CuS (Fig. 3.14) in the space group *P6₃/mmc* (cell constants a = 3.796 A°, c = 16.380 A°; JCPDS 01-078-0876).

(a)   (b)
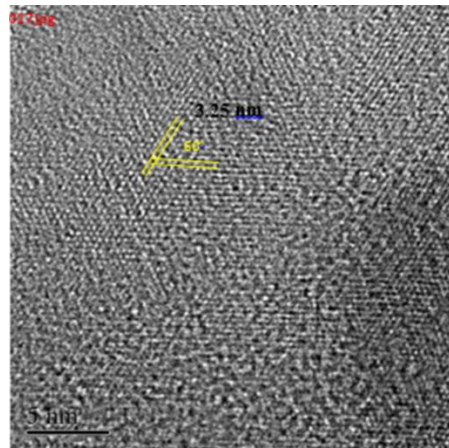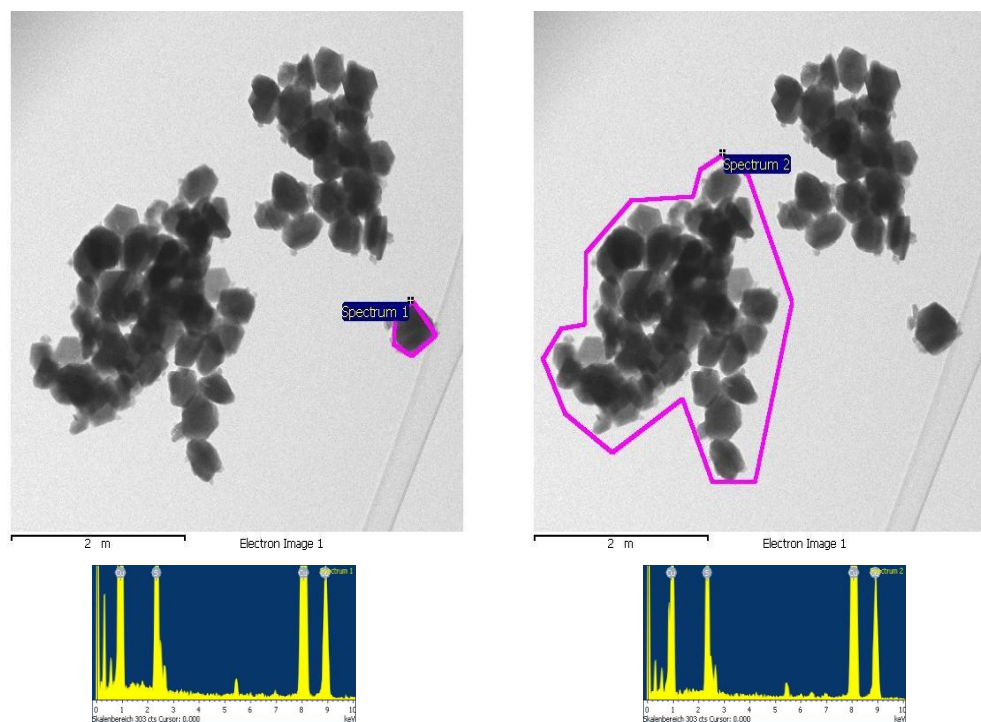
Fig. 3.13: SAED images of CuS

Fig. 3.14: HRTEM image of CuS

## 3.5.3 Characterization of NP.3

The energy dispersive X-rays (EDX) of the sample NP.3 is shown in Fig.3.15. For Cu 66.06 at%, there is contribution of 20at% of Cu from Cu mesh. The atomic % of S is 33.94%. . Eliminating this Cu 20at% from total Cu suggests that Cu and S are present in 1:1 atomic ratio indicating the CuS phase. The larger CuS particles can also be seen due to the agglomeration of smaller particles. The selected area electron diffraction (SAED) analysis of the CuS nanoparticles consists of bright spots which is explaining the crystallinity of the sample. The SAED analysis also confirmed the hexagonal structure observed in the TEM images of the Copper sulfide Nano particles.

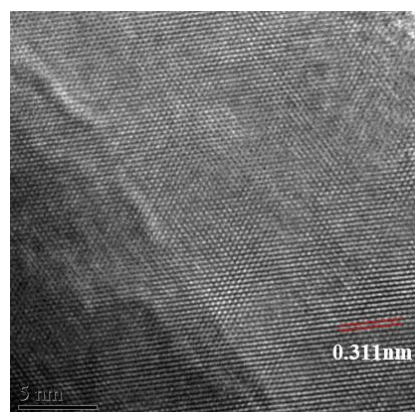| Element	Weight %	Atomic %
S	20.59	33.94
Cu	79.41	66.06
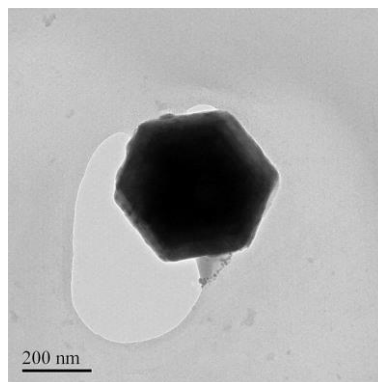
Fig. 3.15: EDS and TEM images of CuS/Cu₂S

The clear distribution of the SAED spots in fig 3.16 indicates the single crystal nature of the nanoparticles. The HRTEM image of Copper sulfide nanoparticles in fig.3.17 shows clear visible lattice fringes and complements the SAED analysis, and provides the evidence of single crystal nature of the CuS nanoparticles. In the HRTEM images, inter planar spacing is found at 0.311 nm which matches with Cu_2S (chalcocite) hexagonal phase. These results shows that a mixed phase of copper sulfide nanoparticles is formed.
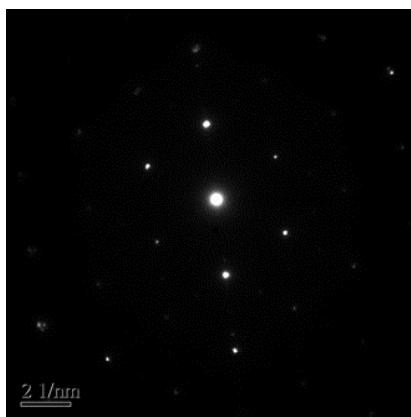

Fig. 3.16: SAED image of CuS/Cu₂S   **Fig. 3.17: HRTEM of CuS/Cu₂S**

3.5.4 Characterization of NP.6

The energy dispersive X-rays (EDX) of the sample NP.6 is shown in Fig.3.18 (d) For Cu 55.38 at%, there is contribution of 20at% of Cu from Cu mesh. The atomic % of S is %. 44.62. Eliminating this Cu 20at% from total Cu suggests that Cu and S are present in 1:1 atomic ratio indicating the CuS phase. Thus, the EDX spectrum of the sample shows the CuS phase without any other impurity.

| (a) | (b) | (c) |

| Element	Weight %	Atomic %
S	28.91	44.62
Cu	71.09	55.38
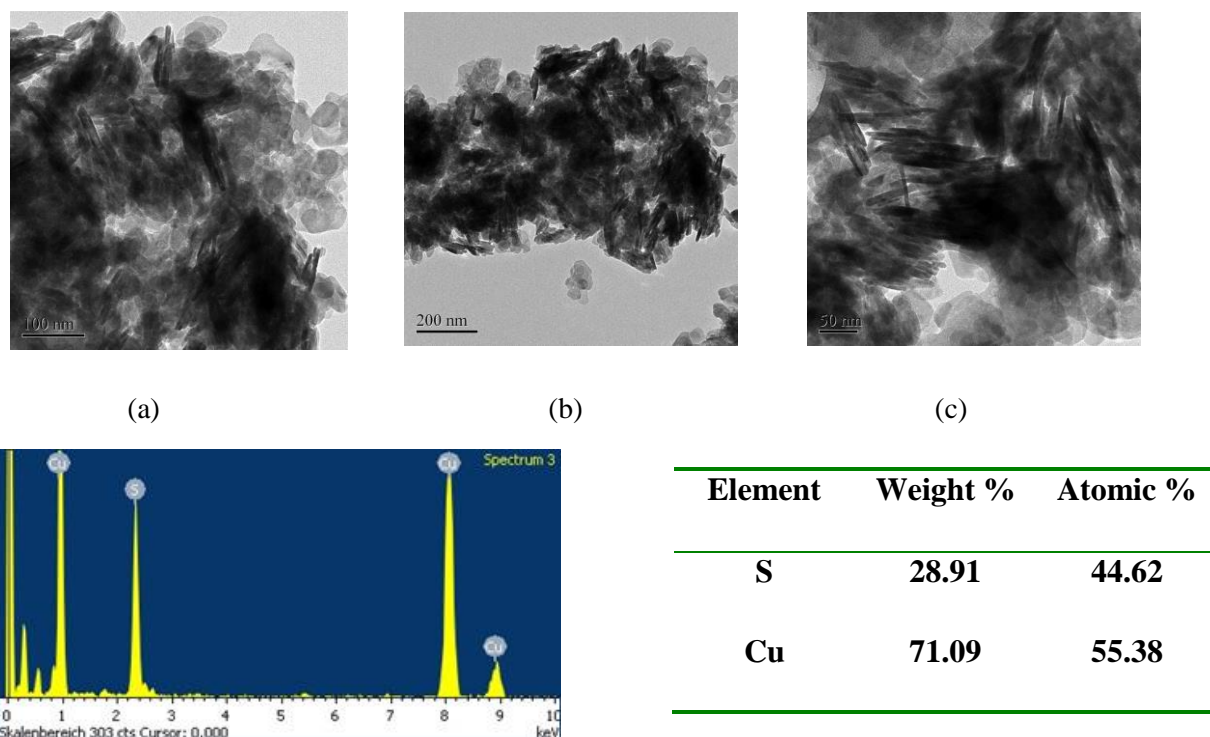
Fig. 3.18: EDS and TEM images of CuS (a-d)

The TEM images at different magnifications are seen in fig.3.18 (a-c) .The larger CuS particles can also be seen due to the agglomeration of smaller particles. The TEM images shows that there also some nanorods of length less than 100nm. The selected area electron diffraction (SAED) analysis of the CuS nanoparticles consists of bright spots which is explaining the crystallinity of the sample. The SAED analysis also confirmed the hexagonal structure observed in the TEM images of the Copper sulfide Nano particles. The clear distribution of the SAED spots in fig 3.19 indicates the single crystal nature of the CuS nanoparticles. The HRTEM image of CuS nanoparticles in fig.3.20 shows clear visible lattice fringes and complements the SAED analysis, and provides the evidence of single crystal nature of the CuS nanoparticles. In HRTEM

images, inter planar spacing is found at 0.327 nm and 0.298 nm which matches with CuS (Covellite) hexagonal and this confirms the formation of hexagonal CuS. [5]
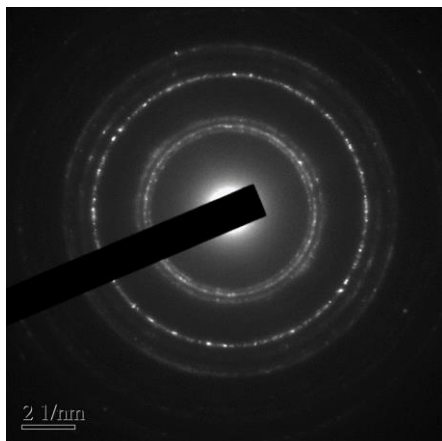
Fig. 3.19: SAED image of CuS
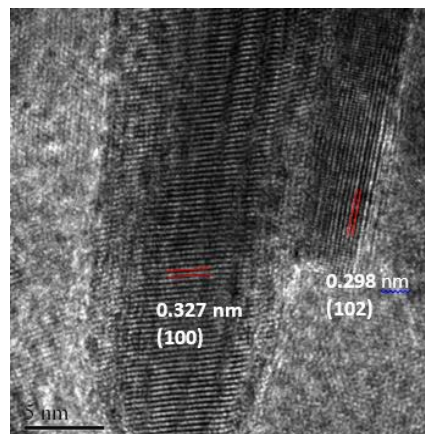
Fig. 3.20: HRTEM of CuS

3.6 Dye degradation studies

3.6.1 NP.5 in Dark, UV and Visible Light

The decolorization of the CR dye in the presence of 0.05 g of NPs is studied using three different treatment processes, that is in dark, under visible and UV light, respectively. For blank experiments in the absence of the catalyst no degradation of the dye took place.

Figs. 3.21, 3.22 and 3.23 show that the process was fast in the beginning but progressively slowed down and then fasten up at the end. The reason is that the dye was first adsorbed on the surface of nanoparticles, with passage of time too much nanoparticles accumulation slowed down adsorption, and the end regeneration of the open nanoparticle surface due to catalytic degradation [9] again fasten the process. In dark fig. 3.21 as there is no source of light that's why only process of adsorption is taking place. This is because of this that it took about 80 min for complete removal of dye in dark. When the dye solution in the presence of CuS nanoparticles was exposed to the visible light and UV irradiation then 100 % of the dye was decolored and degradated after 40 min and 50 min respectively. The UV−vis spectra of the original CR solution and the degraded dye solutions is observed in fig. 3.22 and fig. 3.23. No peak was detected in the analyzed wavelength range at the end of the 40 min and 50 min of reaction time in the presence of CuS under simulated visible light and UV irradiation
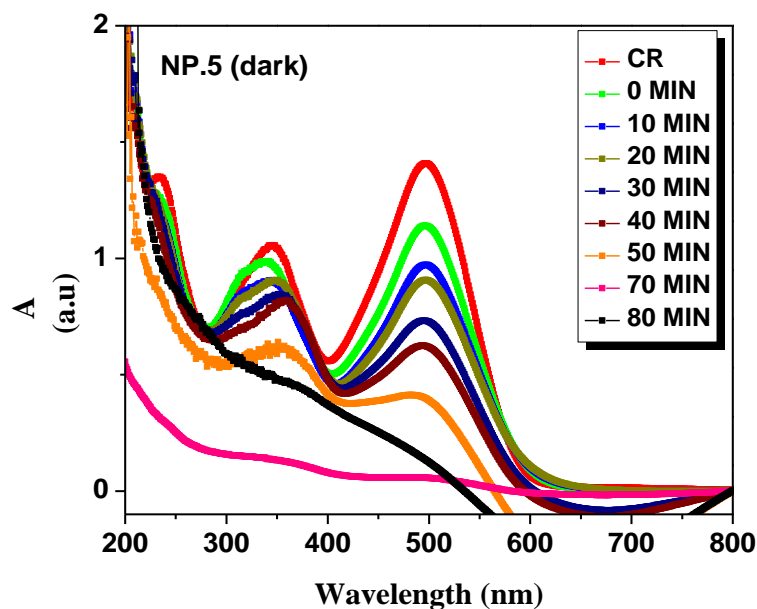
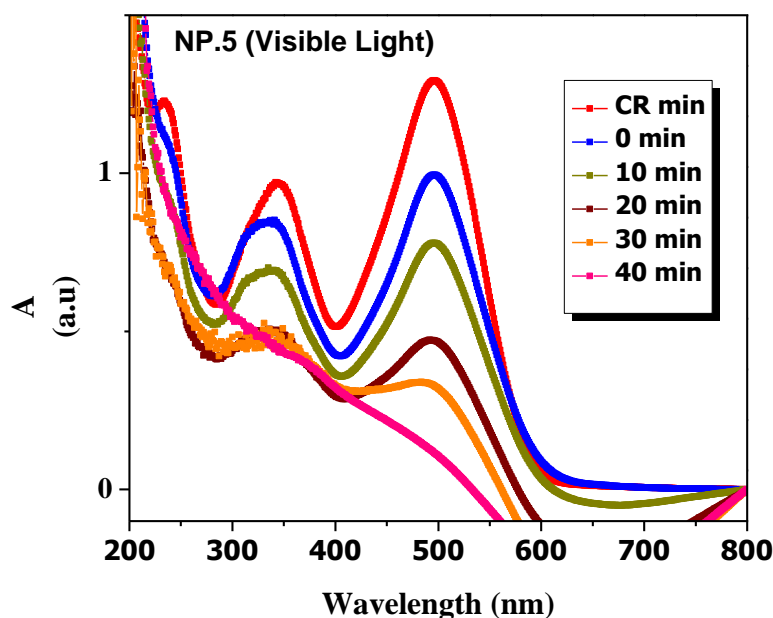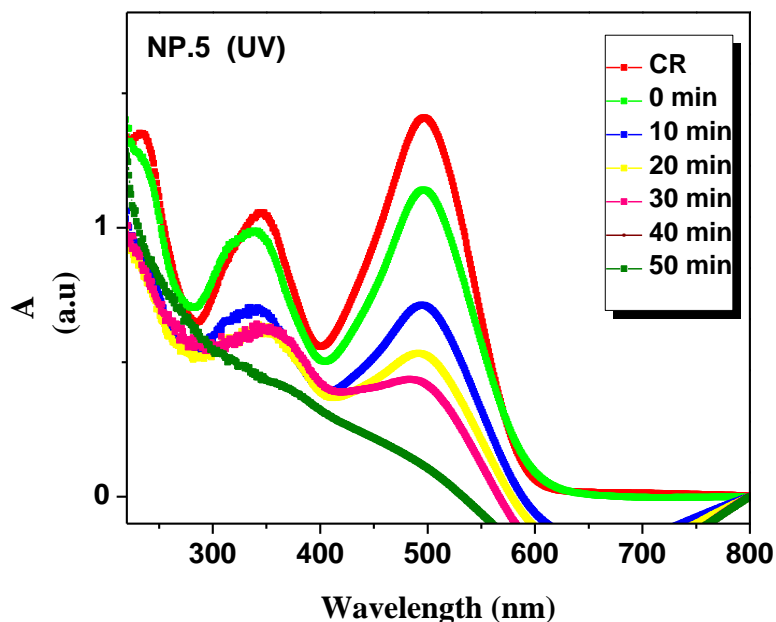**Fig. 3.21: CR degradation by NP.5 in Dark**

Fig. 3.22: CR degradation by NP.5 in Visible Light

As a result, both catalyst and an appropriate light source are necessary for photocatalytic decolorization and degradation of the CR dye on innovative CuS Nanoparticles to occur

To clarify the changes of molecular and structural characteristics of CR as a result of photocatalytic degradation, representative UV–vis spectra changes of the dye solution as a function of reaction time are depicted in figures.

Fig. 3.23: CR degradation by NP.5 in UV

As observed from figures absorption spectrum of the original 100mL CR solution (100ppm) has one main band in the visible region with maximum absorption value at 497 nm and two other bands in the ultraviolet region located at 234 nm and 344 nm, respectively. The Absorbance peaks at 234 nm and 344 nm were due to benzene and naphthalene rings, while the absorbance peak at 497 nm was due to the azo bonds of CR molecule. During photo degradation the absorbance values decline and no more specific peaks are found at 497 nm after reaction. This was due to the degradation of the azo links by attack. In addition to this, the decay of the absorbance at 234 nm and 344 nm were due to degradation of aromatic fragment in the dye molecule and its intermediates.

The full spectrum given in fig. 3.24 showed extremely obvious difference for three different processes. The dye took less time to degrade in presence of visible light but more time was taken by dye to adsorb completely in dark.
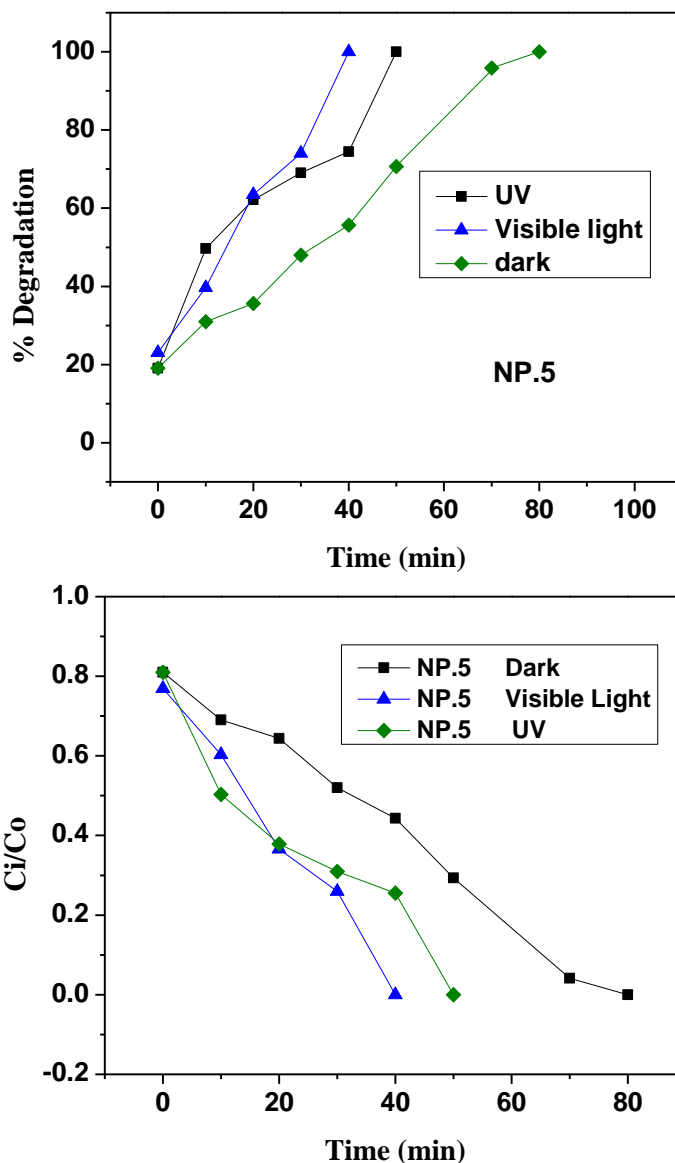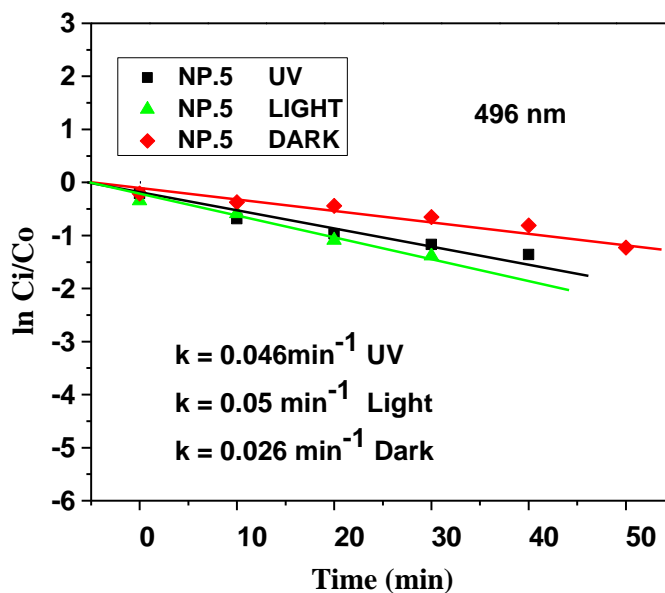
Fig. 3.24: Decrease in Concentration of Dye with Time in dark, UV and visible light
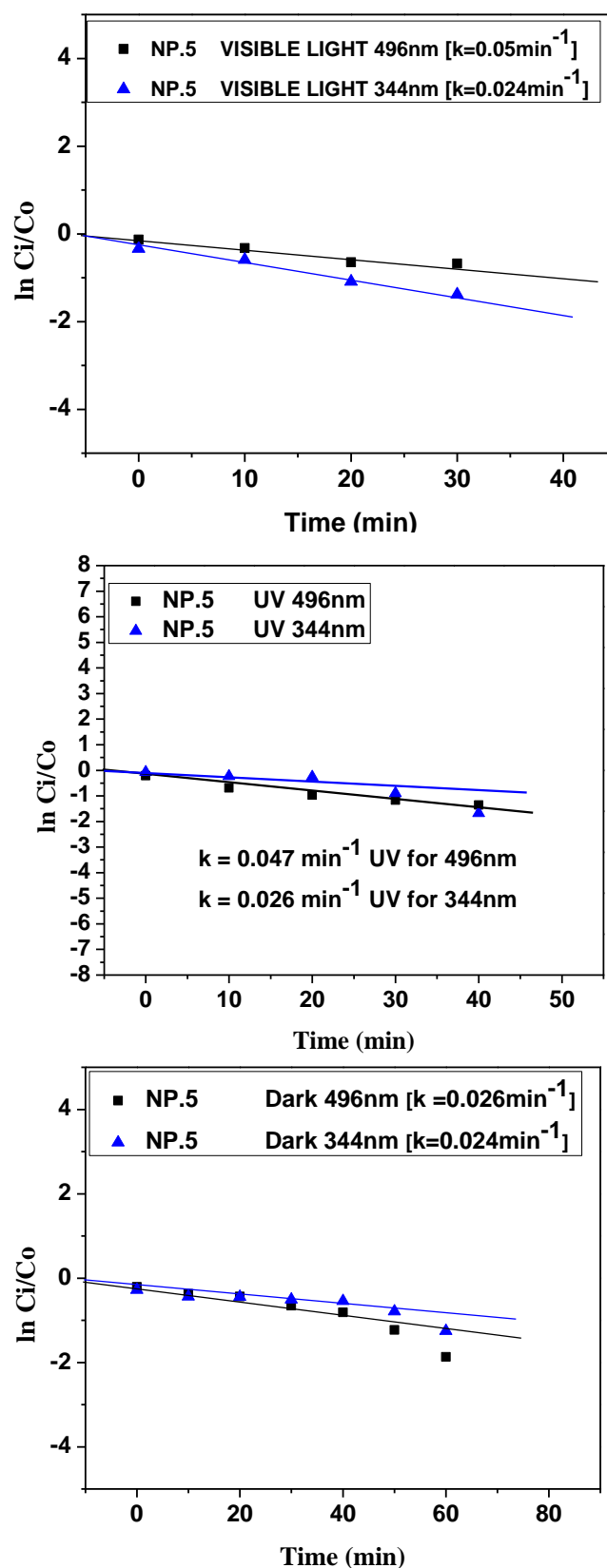
COPPER SULFIDE NANOPARTICLES

Fig.3.25 Pseudo first order kinetics of CR degradation

The rates of three absorption peaks (234nm, 344nm and 496nm) in the presence of CuS Nanoparticles under light, UV and Dark could be compared conveniently in

terms of pseudo first order rate constant from the slopes given in figure 3.25. The absence of graph of 234nm in fig. 3.25 is due to absence of benzene peak. This is because of pi interaction of benzene ring with atoms on the surface of copper sulfide nanoparticles. The faster rate of decay[k= 0.047min^{-1} in UV, 0.05min^{-1} in light and 0.026min^{-1} in dark] of azo group (496nm) as compared to naphthalene group (344nm) was attributed to the priority of cleavage of azo links in the photocatalytic degradation and decolorization. This results in the disappearance of chromophore in the dye structure. The lesser rate constant value for naphthalene (k= 0.026 min^{-1} in UV, 0.024 min^{-1} in light and 0.024 min^{-1} in dark) shows that it will be degraded after azo group. From this we can conclude that not only decolorization but also degradation is taking place. From the graph (1) in fig. 3.25 it is concluded that the rate of reaction is more for the reaction which is taking place in sunlight (0.046min^{-1}) but it is least for the reaction taking place in dark (0.046min^{-1}). These values of rate constants are explaining the speed of the reaction.

3.6.2 Dye Degradation by NP.1 in Dark, Visible Light and UV

The decolorization of the CR dye in the presence of 0.05 g of NPs is studied using three different treatment processes, that is in dark, under visible and UV light, respectively. For blank experiments in the absence of the catalyst no degradation of the dye took place. Figs. 3.26, 3.27 and 3.28 show that the process was fast in the beginning but progressively slowed down and then fasten up at the end.

The reason is that the dye was first adsorbed on the surface of nanoparticles, with passage of time too much nanoparticles accumulation slowed down adsorption, and the end regeneration of the open nanoparticle surface due to catalytic degradation [9] again fasten the process. In dark fig. 3.26 as there is no source of light that's why only process of adsorption is taking place. This is because of this that it took about 90 min for complete When the dye solution in the presence of CuS nanoparticles was exposed to the visible light and UV irradiation then 100 % of the dye was decolored and degradated after 80 min and 60 min respectively. The UV–vis spectra of the original CR solution and the degraded dye solutions is observed in fig. 3.27 and fig. 3.28.
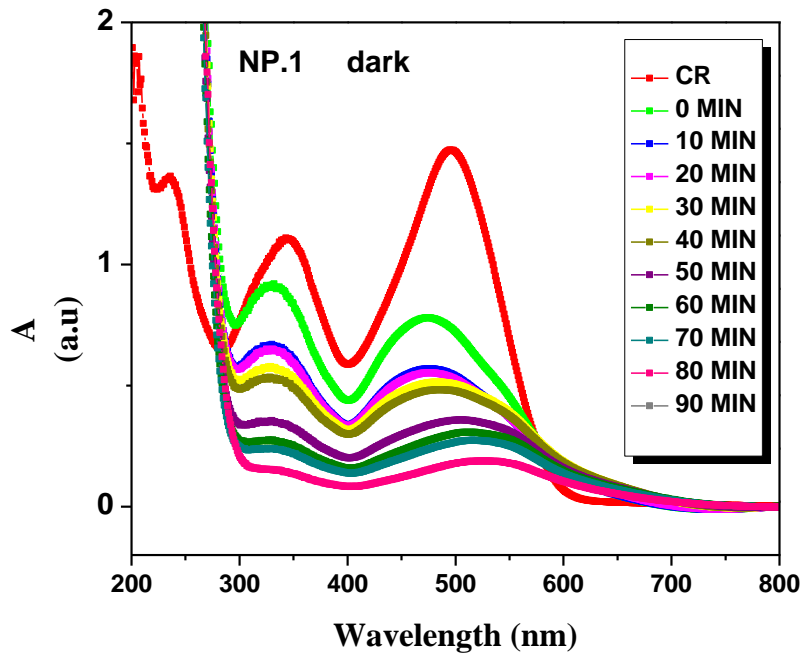
Fig. 3.26: CR degradation by NP.1 in Dark

No peak was detected in the analyzed wavelength range at the end of the 80 min and 60 min of reaction time in the presence of CuS under simulated visible light and UV irradiation. As a result, both catalyst and an appropriate light source are necessary for photocatalytic decolorization and degradation of the CR dye on innovative CuS nanoparticles to occur.
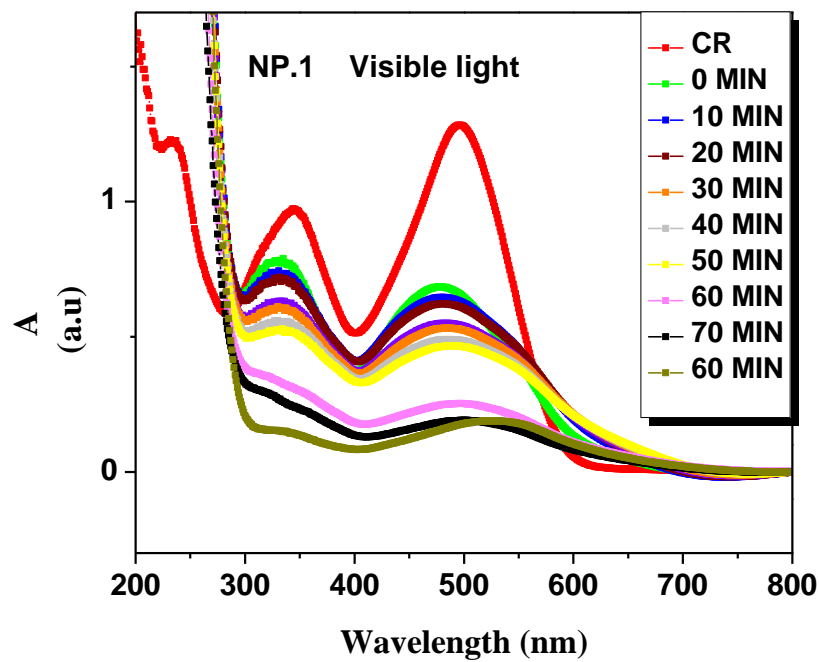

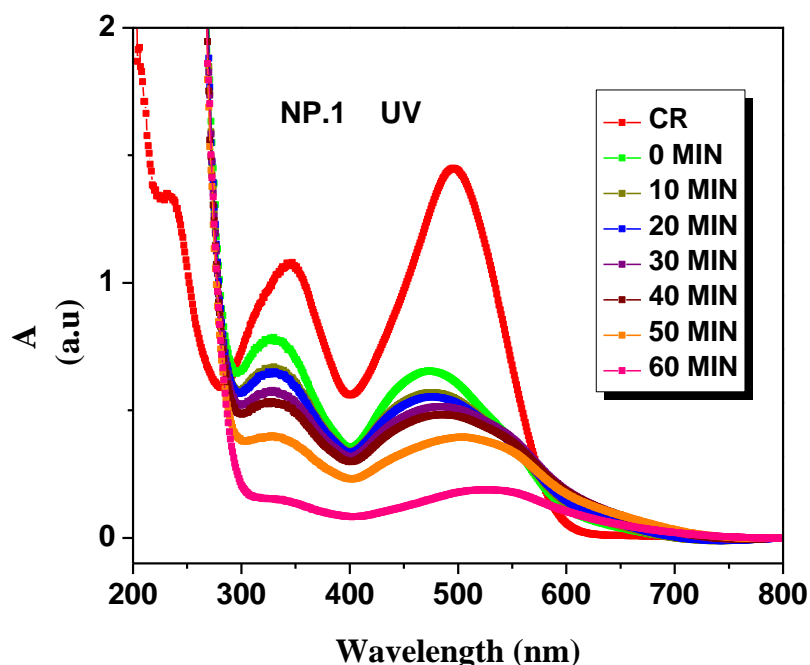**Fig. 3.27: CR degradation by NP.1 in Visible Light**

Fig. 3.28: CR degradation by NP.1 in UV

To clarify the changes of molecular and structural characteristics of CR as a result of photocatalytic degradation, representative UV–vis spectra changes of the dye solution as a function of reaction time are depicted in figures above. As observed from figures absorption spectrum of the original $100mgL^{-1}$ CR solution was characterized by one main band in the visible region with its maximum absorption at 497 nm and by other two bands in the ultraviolet region located at 234 nm and 344 nm, respectively. The Absorbance peaks at 234 nm and 344 nm were attributed to "benzene, naphthalene rings" structures, while the absorbance peak at 497 nm was attributed to the azo bonds of CR molecule. During photo degradation the absorbance values diminish and no more specific peaks at 497 nm remain after reaction, which was due to the fragmentation of the azo links by attack. In addition to this effective bleaching effect, the decay of the absorbance at 234 nm and 344 nm were considered as evidence of aromatic fragment degradation in the dye molecule and its intermediates

The full spectrum given in fig. 3.29 showed extremely obvious difference for three different processes. The dye took less time to degrade in presence of UV light but more time was taken by dye to adsorb completely in dark. The size of nanoparticles NP.4 is less than 60nm, whereas the size of nanoparticles NP. 1 is in micrometers. This is because of this small size (more surface area) that NP.4 has shown better results.
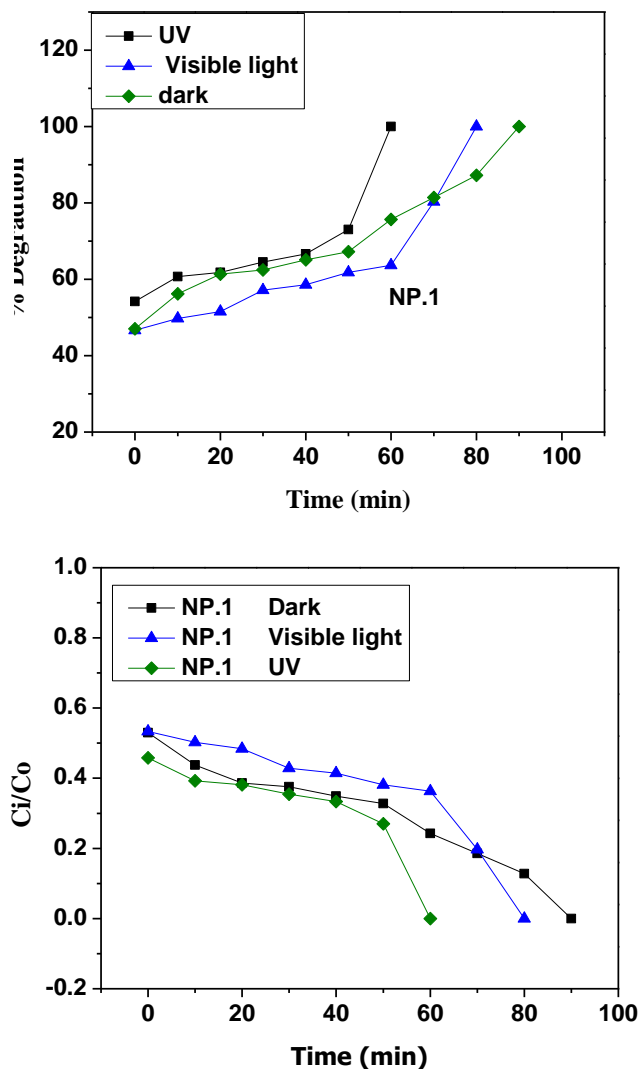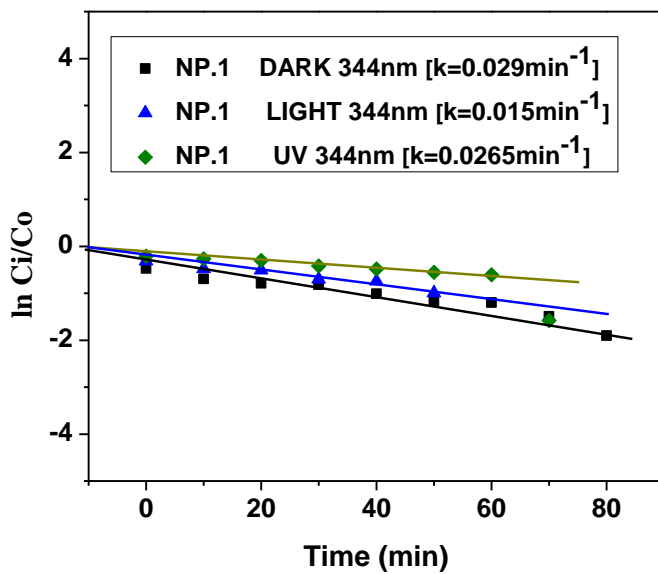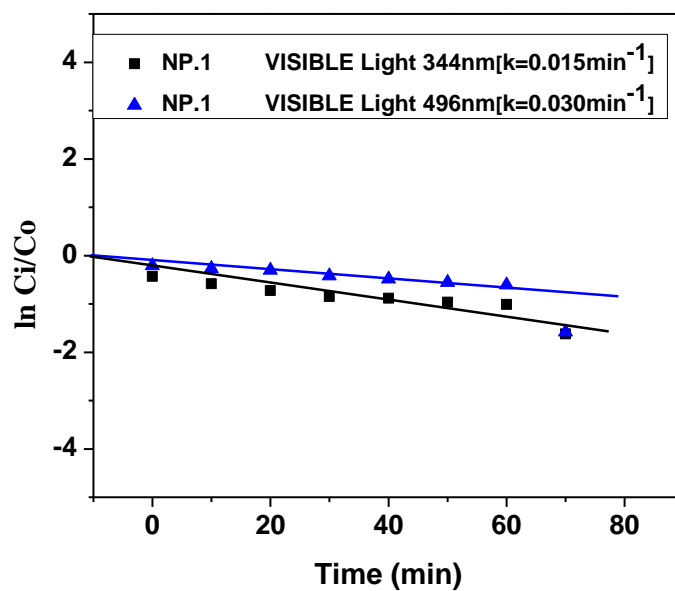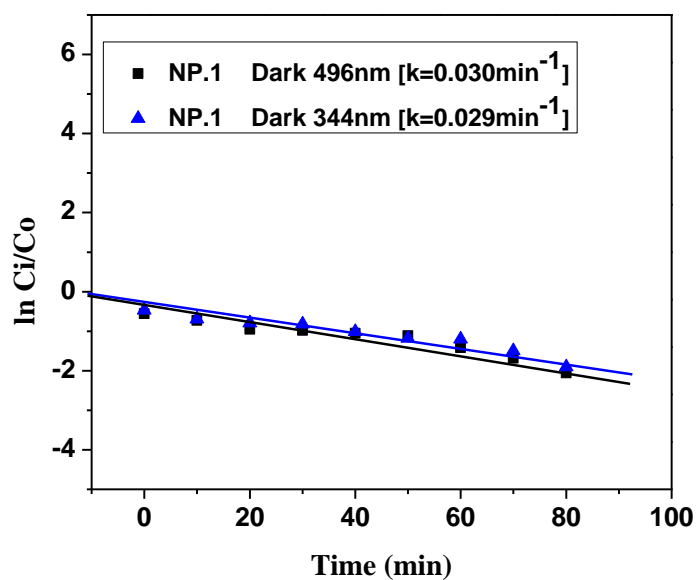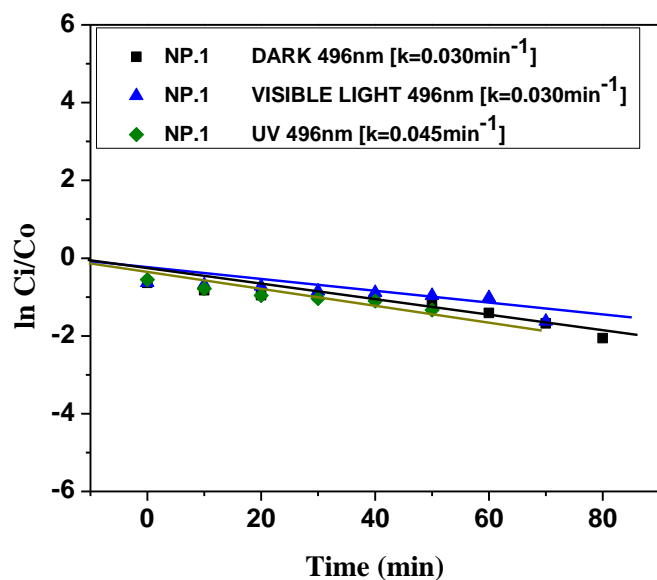
Fig. 3.29: Decrease in Concentration of Dye with Time in dark, UV and light
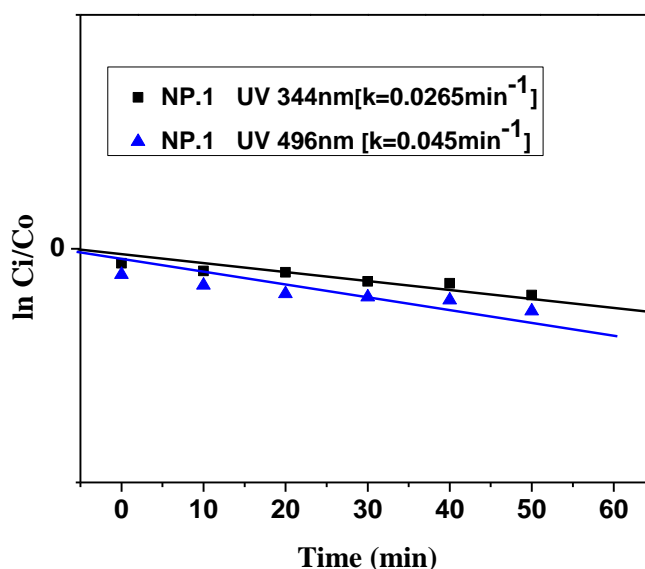
COPPER SULFIDE NANOPARTICLES

Fig. 3.30 Pseudo first order kinetics of CR degradation

The rates of three absorption peaks (234nm, 344nm and 496nm) in the presence of CuS/Cu$_2$S Nanoparticles under light, UV and Dark could be compared conveniently in terms of pseudo first order rate constant from the slopes given in figure 3.30.The absence of graph of 234nm in fig. 3.30 is due to the absence of peak for benzene. This is because of pi interaction of benzene ring with the atoms on the surface of copper sulfide nanoparticles. The faster rate of decay [k= 0.045min^{-1} in UV, 0.030min^{-1} in light and 0.030min^{-1} in dark] of azo group (496nm) as compared to naphthalene group (344nm) was due to the priority of cleavage of azo links in the photocatalytic degradation and decolorization. This results in the disappearance of chromophore in the dye structure. The lesser rate constant value for naphthalene (k= 0.026 min^{-1} in UV, 0.015 min^{-1} in visible light and 0.029 min^{-1} in dark] shows that it will be degraded after azo group. From this we can conclude that not only decolorization but also degradation is taking place. From the graph (1) in fig. 3.30 it is concluded that the rate of reaction is more for the reaction which is taking place in UV (0.045min^{-1}) but it is least for the reaction taking place in dark (0.030min^{-1}). These values of rate constants are explaining the speed of the reaction.

3.6 XRD of nanoparticles after dye degradation

Fig.3.31 is showing the XRD of CuS before and after degradation. Nanoparticles were separated by centrifugation and there XRD was taken. There is no

change in XRD after dye degradation which shows the catalytic properties and stability of nanoparticles. These nanoparticles can be further used for dye removal.
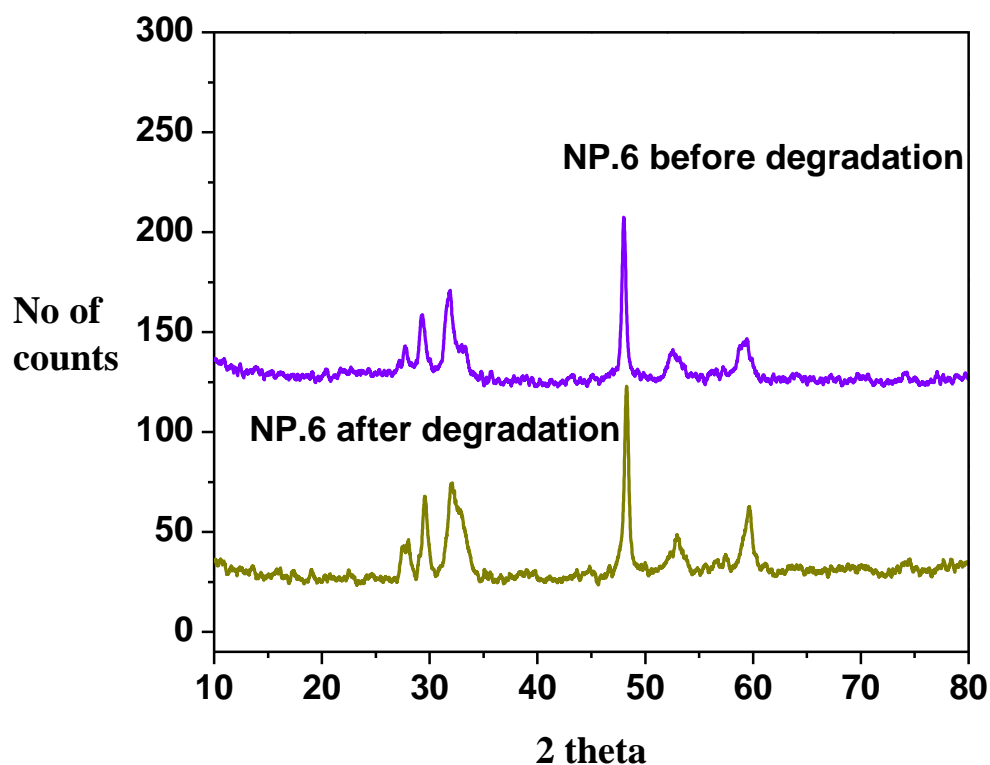

Fig.3.31: XRD of CuS before and after degradation

3.7 Comparison with literature

When dye degradation results were compared with literature [7], it was observed that Copper Sulfide nanoparticles prepared have shown more catalytic activity than those mentioned in the literature. Our synthesized Copper Sulfide nanoparticles have shown 100% degradation in 40 and 70 min in visible light. As compared to this nanoparticles reported in the literature have taken about 135min for complete photo degradation. These Copper Sulfide nanoparticles are very beneficial as they can completely degrade and decolorize the dye even in dark. That's why these are very much good to be used by industries.

CONCLUSION

Copper Sulfide nanoparticles were prepared from copper dithiocarbamate complexes. These nanoparticles were characterized by UV, XRD, TEM and EDS. According to EDS data the synthesized sample was pure. XRD and TEM results revealed the formation of CuS hexagonal nanoparticles from Copper precursors and octylamine and Cu_2S/CuS from copper precursors and ethylene diamine. The size of the nanoparticles prepared from octylamine was less than 100nm whereas the size of the nanoparticles prepared from ethylene diamine was in micrometer. TEM results showed that all of the nanoparticles were hexagonal in shape. H_2S gas was released as a byproduct during the formation of nanoparticles which was trapped by lead nitrate solution to form PbS nanoparticles. Copper sulfide nanoparticles were used to degrade Congo red dye. These nanoparticles degraded the dye in UV, visible light and dark. The process was slow in dark as in that case only adsorption was taking place where as the process was fast in UV and light due to photo degradation process. XRD of nanoparticles after degradation process showed no change in nanoparticles which means that they can be used again and again. Further studies are required to understand the full degradation mechanism.

REFERENCES

1. Ali, R.F; Spectroscopic and X-Ray Single Crystal Characterization of New Bioactive Sulfur Bridged Homobimetallic Copper (II) Dithiocarbamates, 2014

2. Gorai, S; Ganguli, D; and Chaudhuri, S; Synthesis of Copper Sulfides of Varying Morphologies and Stoichiometries Controlled by Chelating and Non chelating Solvents in a Solvothermal Process, Cryst. Growth Des. 5 (2005) 875-877.

3. Lu, Q; Gao, F; and Zhao, D; One-Step Synthesis and Assembly of Copper Sulfide Nanoparticles to Nanowires, Nanotubes, and Nanovesicles by a Simple Organic Amine-Assisted Hydrothermal Process, Nano Lett. 2 (2002) 725-728

4. Jia, B; Qin, M; Jiang, X; Zhang,Z; Zhang,L; Liu,Y; Qu,X; Synthesis, characterization, shape evolution, and optical properties of copper sulfide hexagonal bifrustum nanocrystal, J. Nanopart. Res. 15 (2013) 1469

5. Roy,P; Srivastava, S.K; Low-temperature synthesis of CuS nanorods by simple wet chemical method, Mater. Lett. 61 (2007) 1693–1697

6. Yang, Z.K; Song, L.X; Teng,Y; Xi,J; Ethylenediamine-modulated synthesis of highly monodisperse copper sulfide microflowers with excellent photocatalytic applications, J. Mater. Chem. A. 2 (2014) 20004 - 20009

7. Zhu, H; Jiang, R; Xiao, L; Chang, Y; Guan,Y; Li, X; Zeng, G; Photocatalytic decolorization and degradation of Congo Red on innovative crosslinked chitosan/nano-CdS composite catalyst under visible light irradiation, J.Hazard. Mater. 169 (2009) 933–940

8. Gupta, V.K; Pathania, D; Singh, P; Rathore, B.S; Chauhan, P; Cellulose acetate–zirconium (IV) phosphate nano-composite with enhanced photo-catalytic activity, Carbohyd. Polym. 95 (2013) 434– 440

9. Mondal, G; Bera, P; Santra, A; Jana, S; Mandal, T. N; Mondal, A; Seok, S; and Bera, P; chalcocite (Cu$_2$S) nanocrystals: structural, optical, electrical and photocatalytic properties, New J. Chem. 38 (2014) 4774—4782